CAPTURE AND SPURIOUS TARGET GENERATION DUE TO HARD LIMITING IN LARGE TIME-BANDWIDTH PRODUCT RADARS

Hermann H. Woerrlein

Naval Research Laboratory
Washington, D.C.

December 1969

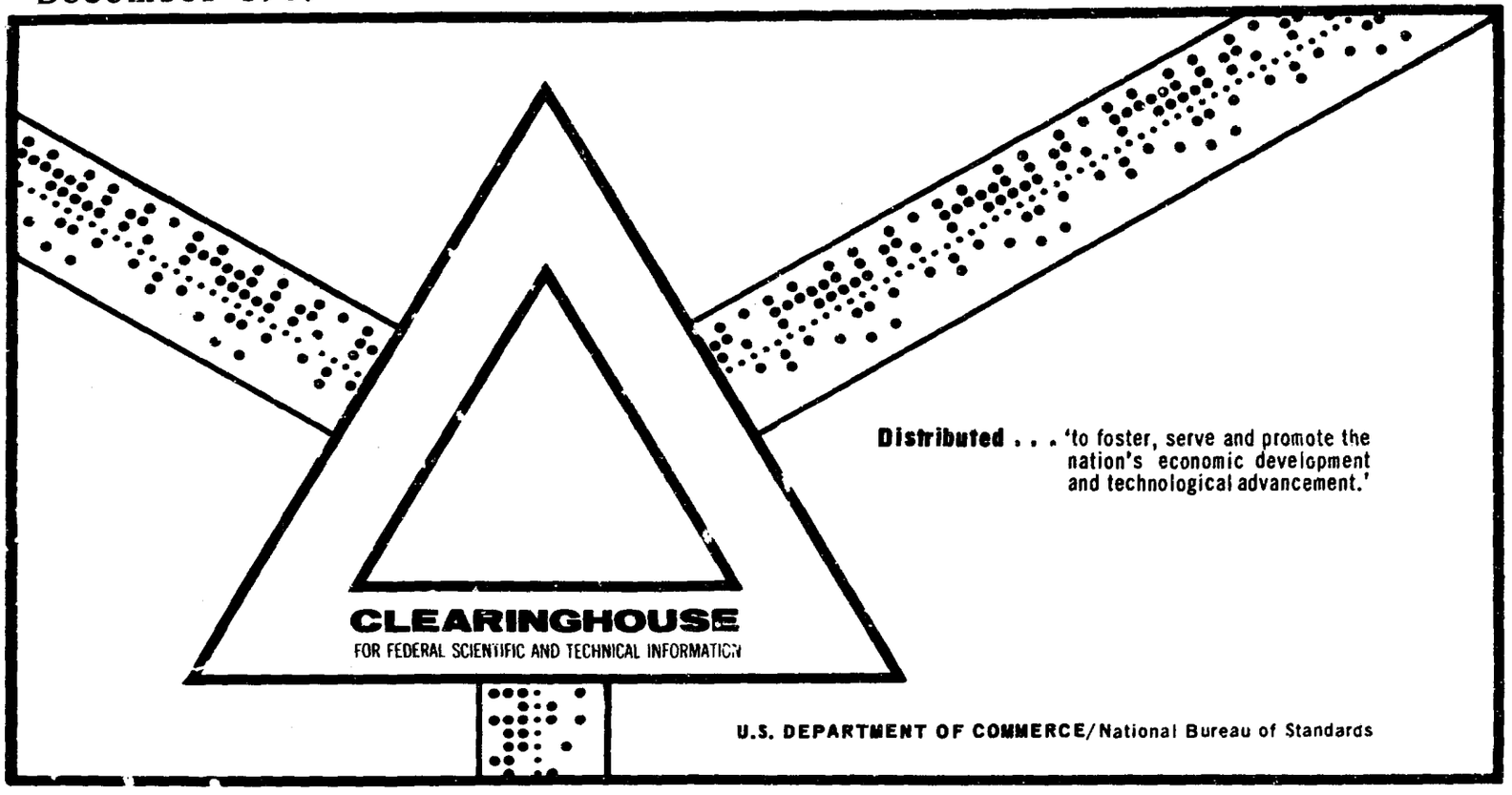

NRL Report 7001

Capture and Spurious Target Generation Due to Hard Limiting in Large Time-Bandwidth Product Radars

HERMANN H. WOERRLEIN

Search Radar Branch
Radar Division

December 22, 1969

NAVAL RESEARCH LABORATORY
Washington, D.C.

CONTENTS

ABSTRACT

Hard limiting before pulse compression or correlation processing is a common approach to the CFAR (constant false alarm rate) problem, and it offers a good and simple solution in a single-target or scarce-target environment. With the advent of radars with a large time-bandwidth product the possibility arises that expanded radar returns due to multiple targets of interest may overlap very largely or entirely but still may be sufficiently separated to be resolved after receiver processing. In this case the compressed pulses cannot attain full amplitude at the processor output even if the signal-to-noise ratio at the input is very high; this phenomenon is known as capture and small signal suppression. The purpose of this report is to exhibit that, in addition to compressed target responses of reduced magnitudes, false targets may be generated with apparent amplitudes of the same order or exceeding those of legitimate targets. Spurious target generation in the case of chirp radar has been known for some time. The theory has been extended to maximum-length linear shift-register codes which are used as modulation functions of pulse-compression and phase-coded CW radars. It is found that a single pair of radar returns coded in this manner is subject to capture only and not to false target generation. Surprisingly, however, the addition of a third expanded signal produces a spurious response. This generation of a false target should be taken in account when the dynamic range of future phase-coded radars using linear shift-register codes is specified, in particular if the radar is designed for automatic track and raid-size determination.

General formulas were derived to predict the effects of capture and false target generation as a function of the signal energy distribution and relative phasing before entering the limiting device. The formulas were evaluated numerically, with the results being presented in the form of computer-generated plots.

PROBLEM STATUS

This is the final report on NRL Problem R02-38.201. The problem will be considered closed 30 days after the issuance of this report.

AUTHORIZATION

NRL Problem R02-38.201
Project S-4614-6173

Manuscript submitted October 8, 1969.

CAPTURE AND SPURIOUS TARGET GENERATION DUE TO HARD LIMITING IN LARGE TIME-BANDWIDTH PRODUCT RADARS

SUMMARY

This report contains the results of a study of the effects of limiting combined with various types of pulse coding in the suppression or "capture" of real targets and the generation of false targets. In the study, the radar return is described by a complex signal vector which is modulated in amplitude and in phase. The limiter generates an output vector in phase with the input vector, but with a constant (unit) amplitude. Throughout this report is is assumed that the limiter input waveform is the sum of two or three phase-coded signals of the same kind but with different delays. The component signals are assumed to overlap entirely. Their amplitudes and the rf phases of their carriers may be arbitrary. It is assumed that the signal-to-noise ratio is high and that the beat products coming out of the limiter can therefore be predicted. It is shown in the different sections of the report how the beat products may interfere with the legitimate target returns, thus causing an apparent amplitude change (capture effect) and how they may combine and form new signals of the same kind as radiated by the radar, thus causing a false target response (spurious target, ghost target).

In the first two sections of the report the model and the assumptions are explained and are related to radar designs. Examples show how limiting takes place in radar receivers. There are two cases: intentional limiting, to obtain CFAR (constant false alarm rate) or to reduce equipment complexity, and accidental limiting, which occurs if the radar receiver is overdriven by large clutter returns or electronic interference.

The sections following the first two sections are devoted to the analysis of the limiter output if the input consists of two or three mutually delayed expanded radar signals. The sections are the following:

1. General Theory of the Hard Limiting of Two Input Signals. In this section general formulas are derived and discussed. The nonlinear relationship between limiter output and the instantaneous phase difference of the input signals is developed into a Fourier series. The Fourier coefficients C_n are calculated for the order n in the range between -14 and +15. The results are plotted and printed out for a number of parameter choices.

2. Limiting of a Pair of Constant-Frequency CW Sinusoids. This section may be of interest to the designers of CW, pulsed CW, or pulse doppler radars. The theory compares favorably with a bench test.

3. Limiting of a Pair of Linearly-Frequency-Modulated Signals. It is shown that in addition to small signal suppression there is a false target generation effect. After pulse compression an array of false targets appears to both sides of the true target returns.

4. Limiting of a Pair of Zero-Pi-Phase-Modulated Signals. All components of the limiter output may be identified with images of the original input signals. The smaller signal will be captured to an amount depending on the intensity ratio before limiting and on the carrier rf phase. The capture effect is minimized if the carriers are 90 degrees out of phase. There is no evidence of any false targets.

5. General Theory of the Hard Limiting of Three Input Signals. The two-signal theory is extended to the three-signal case in a straightforward manner. A two-dimensional Fourier series is used to express the nonlinear relation between output and input quantities.

6. Limiting of a Triplet of Linear Coded Sequences. It is shown that the limiter output is composed in this case of four coherent signals. Three signals are identical with the input signals, and they are the true target responses; but the fourth signal has a pseudo-random delay, and it is a false target or ghost target. The theory is confirmed by the results of a computer simulation. (To be exact regarding the history of this study, the computer simulation was made first, and the theoretical explanation for the false target generation effect was sought and found afterward.) Pseudo-three-dimensional plots show the various captured true target amplitudes and the false target amplitude as a function of the carrier rf phases and with various signal magnitude ratios as parameters. It is seen in this section that the false target may be as strong as the true targets. If there are two equally strong true targets and one smaller true target, there will be a false target of approximately the same size as the smaller true target. The location of the false target changes erratically if the true target geometry changes slightly.

APPROACH

It is assumed that the radar transmits a phase-coded signal of large time-bandwidth product. The phase codes considered in this report are linear FM and linear shift-register-generator sequences, as they are described for example in Ref. 1. The target space contains a number of discrete point scatterers at different ranges; that is, the targets are assumed to be far enough separated that they can be resolved individually by the radar. At the radar receiver input there will therefore be a summation of phase-modulated sine waves, with the phases between the sine waves depending on the very accurate range increments between the multiple targets and with the time delays between the modulation functions depending somewhat less sensitively on the geometry. The summation of the individual radar returns will hence be both amplitude and phase modulated, even if the transmitted signal envelope was constant.

The type of transmitted signal calls for a matched filter or a correlator as a receiver-processor. In practice the receiver-processor is frequently preceded by a hard-limiting device, which may be operating either at IF or on the in-phase and quadrature components of bipolar video signals, depending on the radar design. Examples of such receiver designs are given in the next paragraph. For the purpose of this analysis the hard limiter is assumed to be at IF. The hard limiter at bipolar video can be handled as a special case of the IF limiter, wherein the input signals are allowed to be in phase (positive) or 180 degrees out of phase (negative) and are not allowed to have phase values in between.

To keep the theoretical model as simple as possible without losing significance it is assumed that two or three signals with various relative magnitudes, delays, and RF phases are present at the limiter input. It is also assumed that the noise is negligible at the limiter input. The assumption of a large signal-to-noise ratio may not always be fulfilled, and in such cases the results of this analysis should not be applied. It is well known that the limiter acts like a linear device causing a loss of only 1 to 1.5 dB in radar sensitivity as long as the signals are sufficiently deep in the noise (2,3). This study is concerned with the case that the limiter output signal can be predicted from the radar and the target parameters. In this deterministic case the nonlinearities of the channel cause the formation of coherent beat products which may correlate with the transmitted radar code at a time shift which does not correspond to the actual location of a physical target. In this case a spurious target response is generated. The amplitude of the

spurious target cannot be explained as simply an addition of range side lobes, as would be indicated if linear-matched-filter theory would hold. The false targets may be of the same magnitude or stronger than the true targets. This fairly quantitative claim has been supported by the results of a computer simulation.

Complex signal notation is used throughout this analysis. The limiter is mathematically described as a device which removes the amplitude variation from the complex signal. The limiter output is a complex phase-modulated signal of uniform amplitude. It is assumed that the limiter operates distortion-free, i.e., that the phase modulation of the input signal arrives undistorted at the output. Much of the approach to the problem was influenced by thoughts presented by Nolen in a paper entitled "Effects of Limiting on Multiple Signals" (4). To preserve continuity and also since Nolen's paper is not generally available, some of his results, particularly those pertaining to linear FM, are reviewed in this report.

It may be argued that the signal-to-noise ratio of the unprocessed signal is ordinarily very small in typical pulse-compression or phase-coded CW correlation radar systems of large correlation gain. Therefore the assumption that the signal-to-noise ratio is large would in many cases not be valid and the conclusions from this study would not apply. It is true that the signal-to-noise ratio may be exceedingly small for a minimum detectable signal. One should keep in mind, however, that large interfering scatterers (clutter) may be strong enough to dominate over the noise at the limiter input even if the radar is designed to detect very small signals by virtue of a high correlation gain.

IMPLEMENTATION EXAMPLES OF HARD-LIMITING RECEIVER-PROCESSORS

Hard limiting may take place at IF or at bipolar video, which may also be considered as zero IF. Components of limited dynamic range, like RF amplifiers or mixers, may act very much like hard limiters as soon as they become saturated by large signals. The IF limiter may be considered as a device which ideally would preserve the phase and destroy the amplitude modulation of a signal. If the input signal is mathematically described by a complex vector of variable amplitude and variable rotation rate, then the output signal would be given by a constant-amplitude vector which points at any given moment in the same direction as the input vector. The output vector may be assumed to have unit amplitude all the time. To practically implement a hard-limiting device one may use amplifier chains whose gain is controlled through a feedback loop in such a fashion that it is inversely proportional to the input signal amplitude. At the output of the amplifier chain one would observe a phase-modulated sinusoidal signal with constant amplitude as long as the feedback loop is fast enough to respond to changes of the input amplitude. A probably less troublesome way to achieve hard limiting is to use the cutoff characteristics of suitable nonlinear elements like transistors or diodes, after the input signal has been sufficiently preamplified.

Figure 1 is a simplified diagram of a linear FM pulse-compression receiver. The RF signal coming from the duplexer is preamplified, heterodyned to a conveniently selected IF, passed through a hard limiter and a weighting filter, pulse compressed in an ultrasonic dispersive delay line, detected, and video amplified for display. The weighting filter may serve a dual purpose in this case. It may be used to reduce the range side lobes of the compressed radar signal and to eliminate higher harmonics which may be generated by the diode limiter. In other words it smooths off the corners of the signal coming from the limiter. A typical reason for placing a limiter ahead of the pulse-compression device is to normalize the noise power so that it is possible to set, after pulse compression and rectification, a detection threshold at a computed level to achieve a constant false alarm rate, or CFAR, no matter how strong the noise or interference is

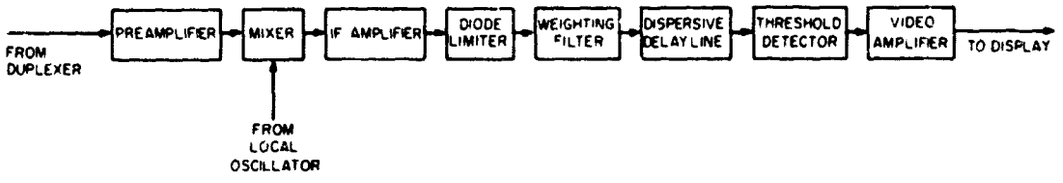

Fig. 1 - Typical linear FM pulse-compression receiver

before limiting. The dynamic range of the radar signal becomes increased through pulse compression by as much as its correlation gain. Limiting may also be used to keep the dynamic range of the processed signal between convenient boundaries. Another reason for limiting may be that it is simpler or cheaper to use components with a relatively small dynamic range and that any large dynamic range after pulse compression would not be needed anyway.

Figure 2 shows a commonly implemented layout for a digital correlator using binary shift registers as memory elements and operating on coherently detected, so called bipolar video signals, the in-phase or I-signal and the quadrature or Q-signal. To reduce equipment complexity one may omit the Q-signal channel. One loses on that case, however, on the average, 3 dB in radar sensitivity. This type of correlator is frequently used to process pseudo-randomly zero-pi-phase-coded radar signals. One of its advantages is its flexibility, since the code memory may contain virtually any sequence of plus and minus bits. The only information that is recorded in the shift registers about the radar signals is the polarity of the bipolar video signals at the instant of sampling. The value of its amplitude is disregarded. The output signals are therefore the same as if hard limiting had taken place in the video amplifiers between the coherent detector and the shift registers in Fig. 2.

GENERAL THEORY OF THE HARD LIMITING OF TWO INPUT SIGNALS

The approach in the case of hard limiting of two input signals is the same as the one selected by Nolen (4). In addition to reviewing the cases of two constant-frequency

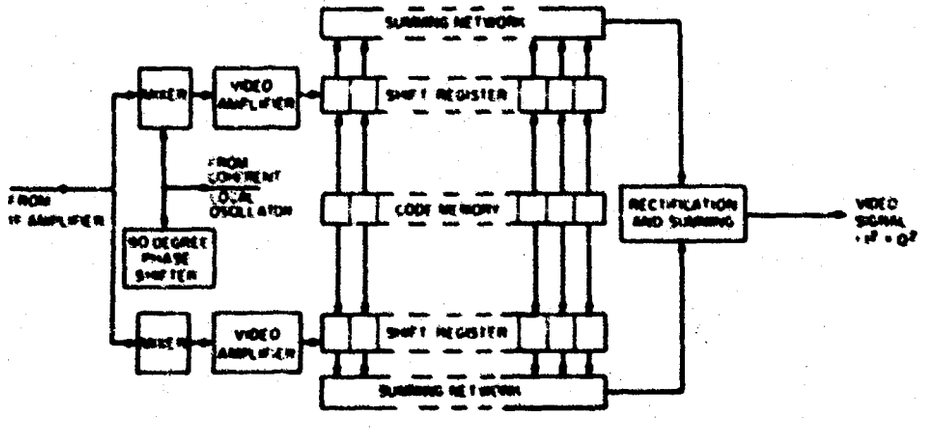

Fig. 2 - Typical digital matched filter layout

sinusoids and two linearly swept FM signals which have been treated by Nolen, a method of handling the case of the pseudo-randomly zero-pi-phase-coded signals by essentially the same technique will be shown.

Two signals at the limiter input may be described mathematically as the summation of two complex vectors. Through separating out a factor $\exp(j2\pi f_0 t)$, where f_0 may be called the carrier frequency, one displays only the variations of the complex vectors with respect to an average position or with respect to a reference vector. In Fig. 3 there is shown as an example two superimposed signals of different magnitudes.

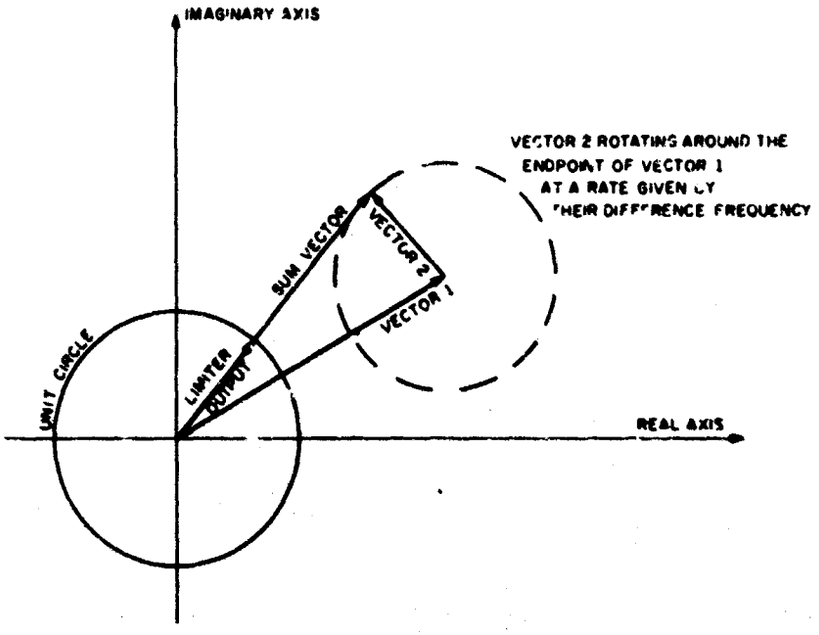

Fig. 3 - Phasor diagram illustrating limiter operation in the complex plane

The signal with the larger amplitude will be arbitrarily designated signal 1. If the vectors represent two sine waves of constant but different frequencies, with f_1 being the frequency of sine wave 1, vector 1 may be considered to be fixed and vector 2 to be rotating with the difference frequency. The true (real) electrical signal may be visualized as the projection on the real axis of the complex vector summation rotated around the origin at the rate f_0.

The heavily drawn vector in Fig. 3 represents symbolically the limiter output signal. Its endpoint always falls on the unit circle around the origin, and it is aligned in parallel with the complex vector resultant from the linear combination of the input signals.

To solve the problem one has to represent the limiter output signal as a function of the phase difference of the input signals with the ratio of the small signal amplitude to the large signal amplitude as a parameter. The evolving nonlinear expression is too complicated to be directly useful, however. Developing the relation between the output signal and the phase change of the input signals in a Fourier series permits a much more useful functional presentation of the output signal in the form of superimposed coherent

phase-modulated signals with amplitudes that can be calculated essentially through evaluation of Fourier coefficients.

Let it be assumed that the limiter input signals have the constant amplitudes A_0 and A_1 and the variable phases $\phi_0(t)$ and $\phi_1(t)$, where t is the time. The input signal s_{in} which is the sum of the two signals would exhibit both amplitude and phase changes as a function of time. By convention the amplitude A_1 shall be no larger than A_0. One can then define the small signal to large signal amplitude ratio a, which would never be larger than 1:

$$a = \frac{A_1}{A_0} \leq 1 \tag{1}$$

The input signal may then be expressed as

$$\begin{aligned} s_{in} &= A_0\, e^{j\phi_0(t)} + A_1\, e^{j\phi_1(t)} \\ &= A_0\, e^{j\phi_0(t)}\left\{1 + a\, e^{j[\phi_1(t)-\phi_0(t)]}\right\} \\ &= A_0\, e^{j\phi_0(t)}\, R\, e^{j\alpha(t)} . \end{aligned} \tag{2}$$

In the last line of this formula, R represents the length of the resultant vector described by the terms between braces on the second line, and α represents its phase. Reference is made to Fig. 4 to explain the relationship. To the end of a unit vector parallel to the real axis is attached a smaller vector of length a and at an angle

$$\theta(t) = \phi_1(t) - \phi_0(t) . \tag{3}$$

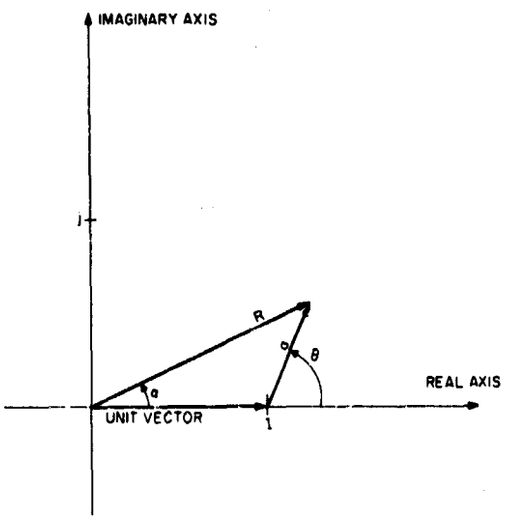

Fig. 4 - Phasor relationships in the complex plane

The action of the ideal limiting device is to replace the time-variable amplitude of the signal by a unit amplitude and to leave its phase untouched. This may be mathematically accompiished by a simple omission of the factors A_0 and R in Eq. (2). The limiter output hence is given by

$$s_{out} = e^{j[\phi_0(t)+\alpha(t)]} . \tag{4}$$

The function α depends on the phase difference θ, which in turn is a function of t. From the geometry depicted in Fig. 4 or through evaluation of the identity

$$R\, e^{j\alpha(\theta)} = 1 + a\, e^{j\theta} , \tag{5}$$

one obtains

$$\alpha = \tan^{-1} \frac{a \sin \theta}{1 + a \cos \theta} . \tag{6}$$

A plot of α as a function of θ and with the parameter a ranging from 0 to 1 in steps of 0.2 is pictured in Fig. 5. If $a = 0$, then α is identically equal to 0. For small values of a, say for $a = 0.2$ the function resembles a sine wave. For $a = 1$, α is a linear sawtooth function connecting from $\alpha = -90$ degrees to +90 degrees and with the discontinuity at $\theta = \pm 180$ degrees. For values of a in the range between 0.2 and 1 the function $\alpha(\theta)$ resembles a distorted sine wave.

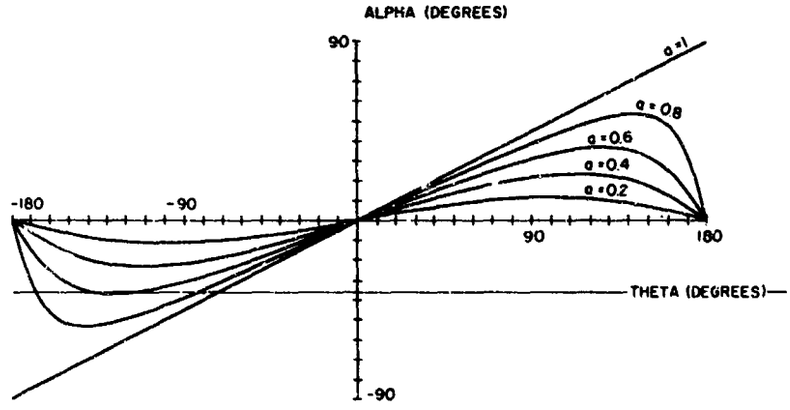

Fig. 5 - Relation between the phase of the sum signal and the phase difference of the component signals

The phase difference θ may change according to a pseudo-random sequence as a function of t, or it may be some other very complicated sequence. Hence the nonlinear expression which one obtains for the output signal through combining Eqs. (4) and (6), namely,

$$s_{out} = \exp j \left[\phi_0(t) + \tan^{-1} \frac{a \sin \theta(t)}{1 + a \cos \theta(t)} \right] , \tag{7}$$

does not directly indicate which signal components are present in s_{out}. In particular it does not show how strongly the original signals are present and whether and to what

extent new signals are generated. It is a fortunate circumstance that the Fourier series development of Eq. (7) leads to a summation whose terms may be identified in several cases of practical importance with images of the input signals and with newly generated signals. Since α is a periodic function of θ with the period 2π, one may use the development

$$e^{j\alpha(\theta)} = \exp\left(j \tan^{-1} \frac{a \sin\theta}{1 + a\cos\theta}\right)$$

$$= \sum_{-\infty}^{+\infty} C_n(a)\, e^{jn\theta} \,. \tag{8}$$

This formula expresses an identity except at those points where the function on the left side has a discontinuity. A finite number of summation terms may provide a very good approximation except in the vicinity of discontinuities. It may be remarked that Eq. (8) does not represent a spectral decomposition of the limiter output but rather a series expansion for a nonlinear relationship.

All coefficients $C_n(a)$ are real, since α is an odd function of θ. The proof is as follows: As a consequence of the relationship $e^{j\alpha(-\theta)} = [e^{j\alpha(\theta)}]^*$, where the asterisk indicates complex conjugate, one may equate $\Sigma C_n(a)\, e^{-jn\theta}$ and $[\Sigma C_n(a)\, e^{jn\theta}]^*$. Hence $C_n(a) = C_n^*(a)$; i.e., the coefficients C_n are real. In the general case the coefficients C_n and C_{-n} will not be the same, however.

Nolen has shown how the coefficients C_n may be obtained by collection of terms from an infinite product of infinite series in powers of $\exp(j\theta)$. It is possible to calculate the C_n values through numerical integration methods, which may perhaps be more easily adapted to automatic computer evaluation. The coefficients may be obtained in the usual way through multiplication of Eq. (8) with $\exp(-jm\theta)$ and integration over θ:

$$\int_{-\pi}^{+\pi} e^{j[\alpha(\theta)-m\theta]}\, d\theta$$

$$= \int_{-\pi}^{+\pi} \sum_{n=-\infty}^{+\infty} C_n(a)\, e^{jn\theta}\, e^{-jm\theta}\, d\theta$$

$$= \sum_{n=-\infty}^{+\infty} C_n(a) \int_{-\pi}^{+\pi} e^{j(n-m)\theta}\, d\theta$$

$$= 2\pi C_m(a) \,. \tag{9}$$

Hence

$$C_n(a) = \frac{1}{2\pi}\int_{-\pi}^{+\pi} e^{j[\alpha(\theta)-n\theta]}\, d\theta \,. \tag{10}$$

This integral may be decomposed into a real and an imaginary part:

$$\frac{1}{2\pi}\int_{-\pi}^{+\pi} \cos\,[\alpha(\theta) - n\theta]\, d\theta + j\,\frac{1}{2\pi}\int_{-\pi}^{+\pi} \sin\,[\alpha(\theta) - n\theta]\, d\theta \,. \tag{11}$$

The second integral is equal to 0, since α is an odd function of θ. By the same token the remaining integral taken from $\theta = -\pi$ to $\theta = +\pi$ is equal to twice the integral taken from $\theta = 0$ to $\theta = \pi$:

$$C_n = \frac{1}{2\pi}\int_{-\pi}^{+\pi} \cos\,[\alpha(\theta) - n\theta]\; d\theta$$

$$= \frac{1}{\pi}\int_{0}^{\pi} \cos\,[\alpha(\theta) - n\theta]\; d\theta\ . \tag{12}$$

Inserting Eq. (6) for α as a function of θ leads to the full expression for the C_n values:

$$C_n = \frac{1}{\pi}\int_0^{\pi} \cos\left(\tan^{-1}\frac{a\sin\theta}{1 + a\cos\theta} - n\theta\right) d\theta\ . \tag{13}$$

Although this integral cannot be evaluated in closed form for any arbitrary value of the signal amplitude ratio a, it can be integrated in the special case $a = 1$. In this case one obtains

$$\alpha(\theta) = \tan^{-1}\frac{\sin\theta}{1 + \cos\theta} = \tan^{-1}\frac{2\sin\frac{\theta}{2}\cos\frac{\theta}{2}}{2\cos^2\frac{\theta}{2}}$$

$$= \tan^{-1}\frac{\sin\frac{\theta}{2}}{\cos\frac{\theta}{2}} = \frac{\theta}{2}\ . \tag{14}$$

This is the equation for the straight line which appears in Fig. 5 if the parameter a is equal to 1. Inserting Eq. (14) into Eq. (12) leads to

$$C_n(1) = \frac{1}{\pi}\int_0^{\pi} \cos\left(\frac{\theta}{2} - n\theta\right) d\theta = \frac{2}{\pi}\frac{(-1)^n}{1 - 2n}\ . \tag{15}$$

Also if $a = 0$, i.e., if the smaller signal disappears entirely, a trivial solution exists. In that case α is identically equal to 0 and one obtains

$$C_n(0) = \frac{1}{\pi}\int_0^{\pi} \cos n\theta\, d\theta = 1\ , \quad \text{if } n = 0\ ,$$
$$= 0\ , \quad \text{for all other } n \text{ values}\ . \tag{16}$$

The general shape of the curves in Fig. 5 suggests that a sine function might be a reasonably good approximation for $\alpha(\theta)$ as long as a is small enough. Analytically one may derive from Eq. (6) that a good approximation is

$$\alpha = a\sin\theta\ , \tag{17}$$

for small values of a. Inserting this approximation into the integral for C_n leads to

$$\frac{1}{\pi}\int_0^{\pi} \cos\,(a\sin\theta - n\theta)\; d\theta\ . \tag{18}$$

This is an integral representation of a Bessel function of the first kind of the order n and with the argument a (Ref. 5).

A good approximation to C_1 and C_{-1} for sufficiently small values of a is therefore $C_1 = J_1(a)$ and $C_{-1} = J_{-1}(a)$. From the first term of the McLaurin series for $J(x)$ one obtains the approximate relationships

$$C_{-1} = -a/2 \quad \text{and} \quad C_1 = a/2, \quad \text{if } a \ll 1 . \tag{19}$$

It would be erroneous, however, to regard Eq. (18) as an approximation for the higher order coefficients C_n. The higher order coefficients C_n depend very critically on the higher order terms in the development of α as a function of θ, and exactly those have been neglected in the approximation given as Eq. (17). A valid approximation may be expressed as a summation of products of Bessel functions (4).

The approximate expression given as Eq. (19) along with the special result given as Eq. (15) provides some insight into the general behavior of the Fourier coefficients C_n as functions of a. A numerical method based on a fast Fourier transform computer program has been used to obtain numerical answers for a set of different parameters. The computer program and the methods by which it was checked are explained in the Appendix of this report. The results are presented as a set of curves in Fig. 6 and in the form of line spectra in Fig. 7. Figure 7 also exhibits digital printouts for the C_n values. The following section of this report will illuminate the physical significance of the Fourier coefficients C_n in a special case.

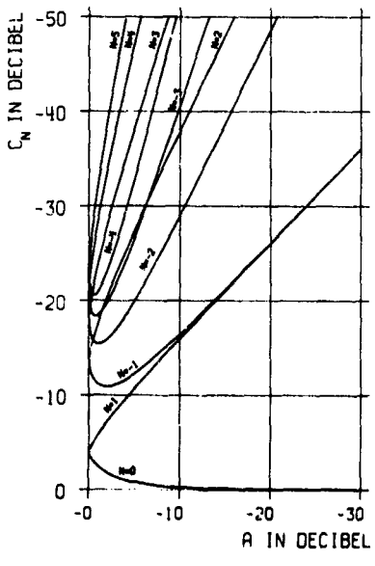

Fig. 6 - The Fourier coefficients C_n as functions of the signal intensity ratio a (labeled A by the computer) and of the order n (labeled N) ranging between -4 and 5

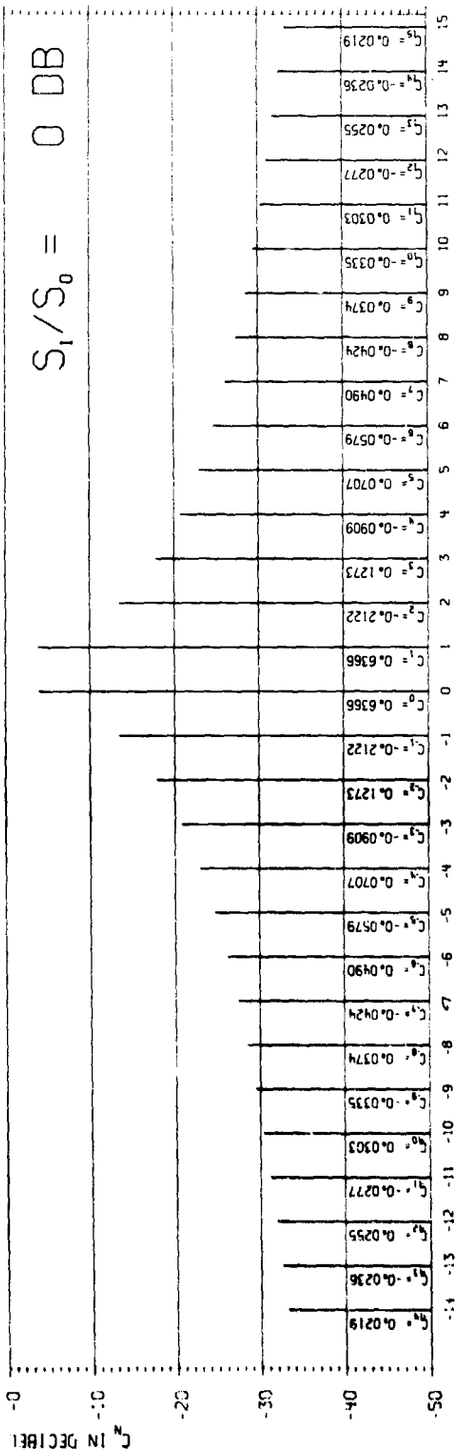

Fig. 7(a) – Spectral line presentation of the Fourier coefficients C_n with the order n between -14 and 15 and strength above -50 dB. The ratio S_1/S_0 = 0 dB is the parameter a expressed in decibels.

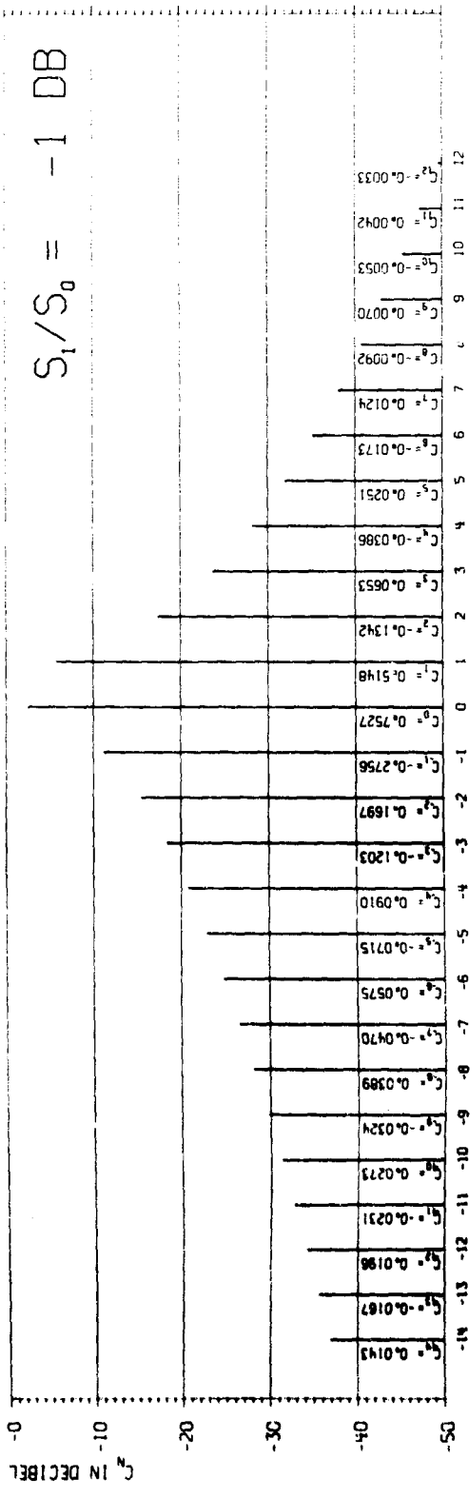

Fig. 7(b) – Spectral line presentation of the Fourier coefficients C_n with the order n between -14 and 15 and strength above -50 dB

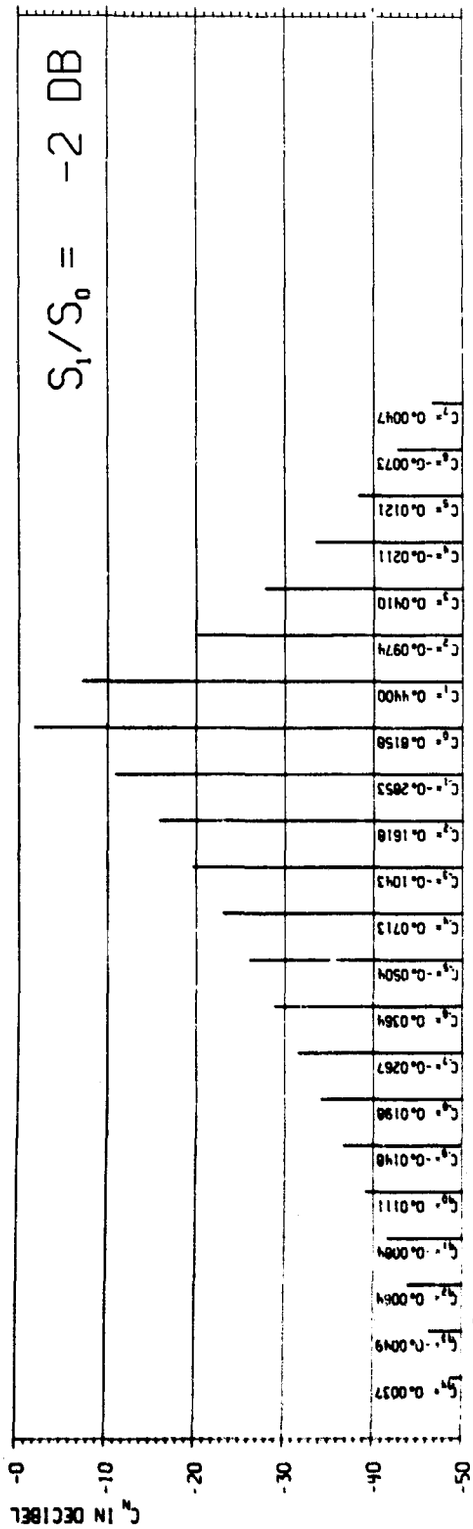

Fig. 7(c) – Spectral line presentation of the Fourier coefficients C_n with the order n between -14 and 15 and strength above -50 dB

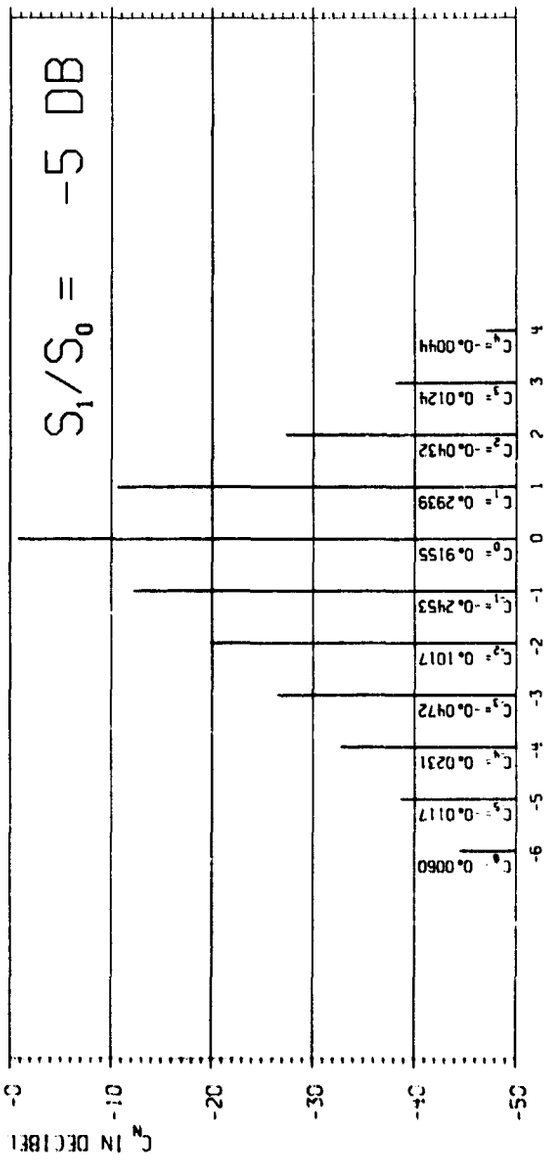

Fig. 7(d) – Spectral line presentation of the Fourier coefficients C_n with the order n between -14 and 15 and strength above -50 dB

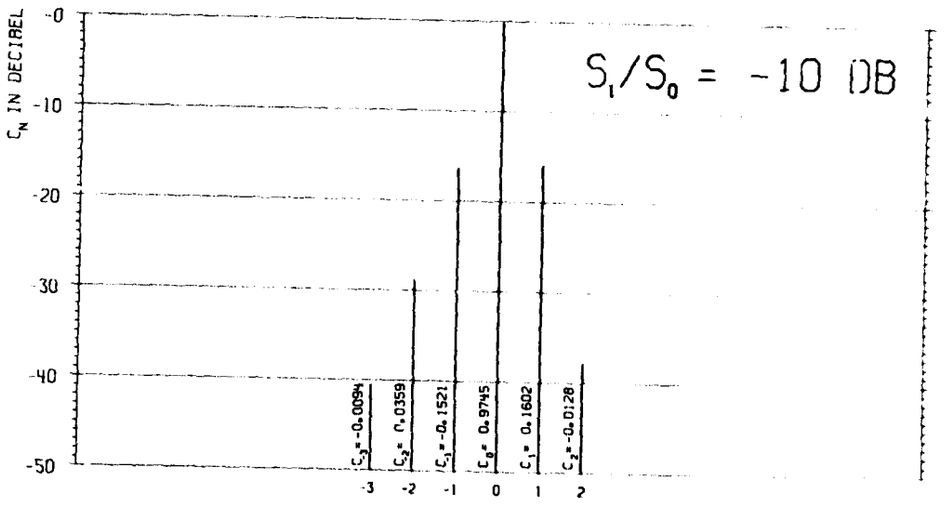

Fig. 7(e) - Spectral line presentation of the Fourier coefficients c_n with the order n between -14 and 15 and strength above -50 dB

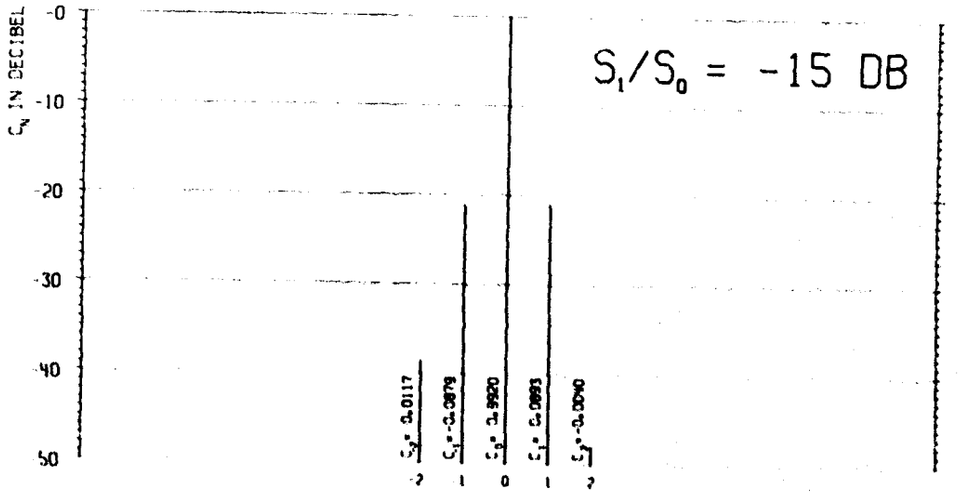

Fig. 7(f) - Spectral line presentation of the Fourier coefficients c_n with the order n between -14 and 15 and strength above -50 dB

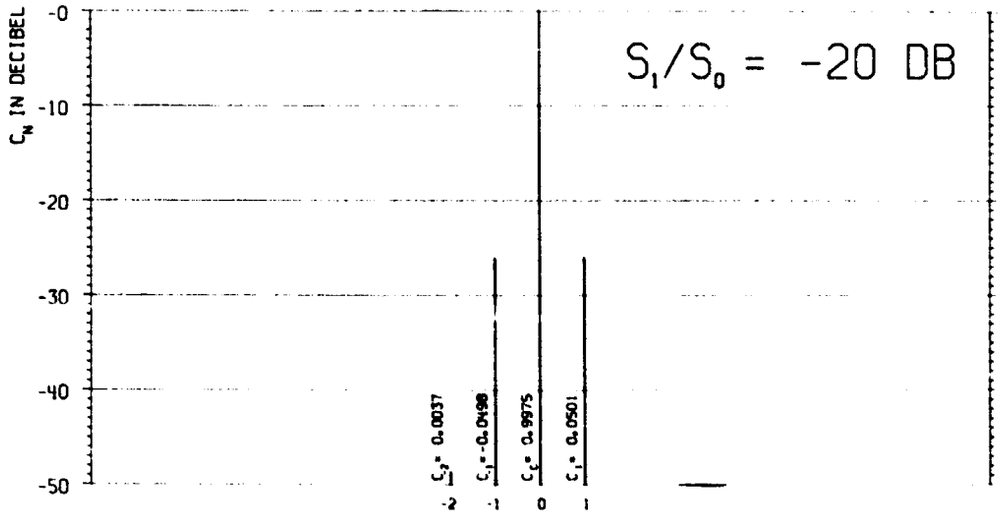

Fig. 7(g) - Spectral line presentation of the Fourier coefficients C_n with the order n between -14 and 15 and strength above -50 dB

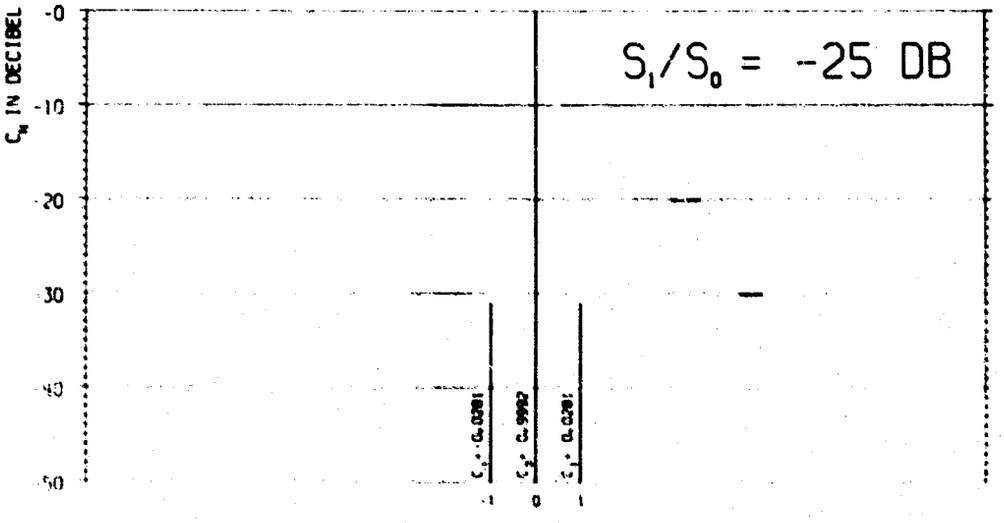

Fig. 7(h) - Spectral line presentation of the Fourier coefficients C_n with the order n between -14 and 15 and strength above -50 dB

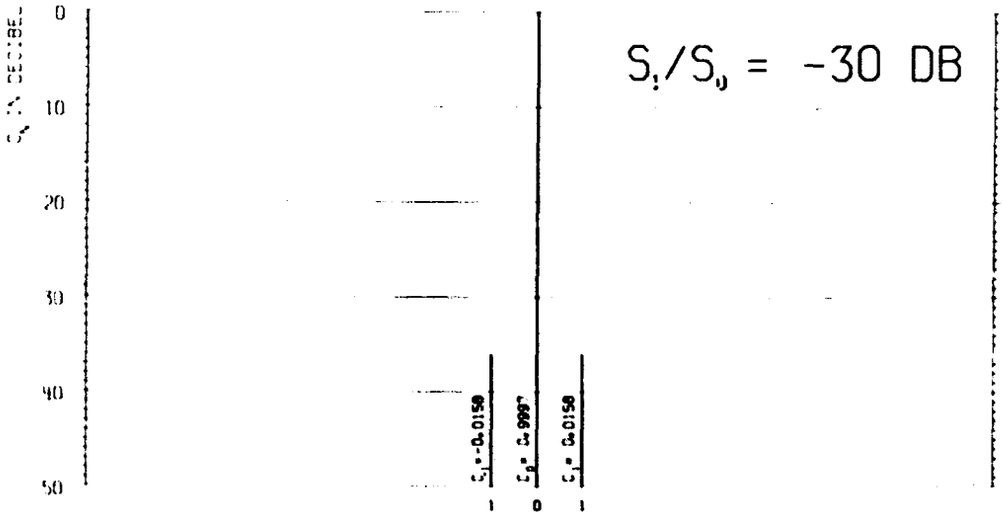

Fig. 7(i) - Spectral line presentation of the Fourier coefficients C_n with the order n between -14 and 15 and strength above -50 dB

An expression for the limiter output signal which will later prove to be quite useful will be derived. The combination of Eqs. (3), (4), and (8) results in

$$s_{out}(t) = \sum_{n=-\infty}^{+\infty} C_n \, e^{j[n\phi_1(t)-(n-1)\phi_0(t)]} \tag{20}$$

where the coefficients C_n are the Fourier coefficients which have been discussed in this section.

LIMITING OF A PAIR OF CONSTANT-FREQUENCY CW SINUSOIDS

The phases of two input signals that are constant-frequency CW sinusoids can be expressed through two linear functions of time:

$$\phi_0(t) = 2\pi f_0 t \quad \text{and} \quad \phi_1(t) = 2\pi f_1 t + \phi_{10} , \tag{21}$$

where f_0 and f_1 are the constant frequencies of the sinusoids, ϕ_{10} is the phase shift which exists at the moment $t = 0$, and the small to larger signal amplitude ratio is given by the parameter a which has been defined in Eq. (1).

Insertion of Eq. (21) into Eq. (20) permits one to write an expression for the limiter output:

$$s_{out}(t) = \sum_{n=-\infty}^{+\infty} C_n \, e^{j[2\pi[f_0 t + n(f_1 - f_0)t] + n\phi_{10}]} \tag{22}$$

This is an expression for a linear superposition of constant-frequency sinusoids, consisting of frequency f_0 with amplitude $C_0(a)$, frequency f_1 with amplitude $C_1(a)$, and sidebands arranged on both sides of the pair of input frequencies at regular intervals determined by the frequency difference $f_1 - f_0$ and with amplitudes tapering off and given by

$C_2, C_3, C_4, \ldots$ on the side adjacent to f_1 and given by $C_{-1}, C_{-2}, C_{-3}, \ldots$ on the other side. Consequently Fig. 7 may be regarded as line spectra of the limiter output waveforms in the case of two monochromatic input oscillations with different frequencies. The figure shows how the spectral envelope becomes distorted unsymmetrically unless the two input signals are equally intense. It should also be noted from Fig. 7 that the higher order beat products (n farther from 0) fall off much faster for small a values (s_1/s_0 closer to 0 db) than for a values in the vicinity of 1. It is evident that the smaller signal may be suppressed relative to the larger signal by as much as approximately 6 dB, as it is well known (6).

It can be seen directly from Eq. (19) that the amplitude ratio of the smaller and the much larger signal after limiting is equal to

$$\frac{C_1(a)}{C_0(a)} \approx \frac{a}{2}, \quad \text{with } a < 1 \tag{23}$$

That is 1/2 the amplitude ratio before limiting. The factor 1/2 in amplitude corresponds to -6.02 dB. The smaller signal is accompanied by a mirror image of approximately the same size.

It is also possible to explain the 6-dB suppression of a small signal without going into mathematics. The small signal may be visualized as a small vector attached to the endpoint of the larger signal vector. The vector resultant from the summation of both input vectors equals the large signal vector with a small additional amplitude and phase modulation caused by the smaller signal. Half of the small signal energy produces the amplitude modulation and half produces the phase modulation of the signal superposition. After limiting, the signal energy is normalized and the amplitude modulation is removed, which would account for a 3-dB loss. The phase modulation is contained in two sidebands, namely in the captured small signal and in its image. Both are of approximately the same intensity and thus suffer a power splitting, which accounts for another 3-dB loss in the power balance.

A simple bench test has been run by R. M. Crisler to check on the validity of the theoretical results described in this section. Two constant-frequency sine waves of high spectral purity, one at 60 MHz and the other one at 60.016 MHz were added together in a hybrid circuit, amplified in an intentionally strongly overdriven and hence hard-limiting IF strip and displayed and photographed on a Singer Model SPA-100 microwave spectrum analyzer. The amplitude ratio a of the two sinusoids could be adjusted by means of a calibrated attenuator inserted in the 60.016-MHz signal path before the hybrid. The IF amplifier may be assumed to have a fairly flat amplitude response over the frequency interval of interest. Figure 8(a) shows the signal superposition before entering the IF strip as it appeared on the screen of a Tektronix type 454 oscilloscope. In Fig. 8(b) is a display of the amplifier output, which exhibits fairly constant amplitude except in the immediate vicinity of the nulls of the input signal envelope. When the input signals differed by a few decibels, the minima of the unlimited signal envelope were large enough to saturate the IF amplifier so that one would observe a constant amplitude oscillation without any dips in the output. Figures 8(c) through 8(j) show the results of the spectral analysis of the linearly superimposed sinusoids (Fig. 8(c)) and of the hard-limited signals (the rest of the pictures). The vertical scale is linear in decibels, each division corresponding to a 10-dB step. Figure 8(c) shows that the input frequencies are free from spurious sidebands before they enter the limiter. In Fig. 8(d) one sees a symmetrical array of spectral lines generated on both sides of the equally strong input frequencies. It should be remarked that the amplitudes of the signal frequencies f_0 and f_1 are approximately 4 dB below the intensity provided by the limiter for a single input signal (compare Fig. 8(d) with Fig. 8(j)).

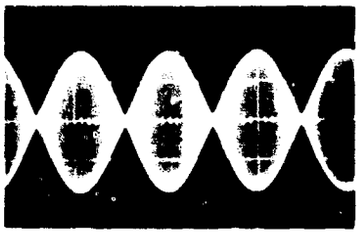

(a) Scope picture of two equally strong sinusoidal signals before limiting

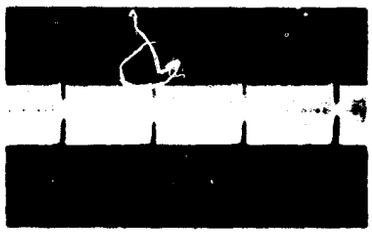

(b) Scope picture of the same signals as in Fig. 8(a) but after hard limiting

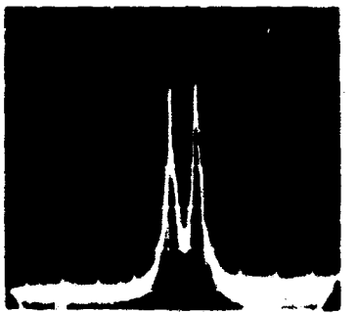

(c) Spectrum of the signals of Fig. 8(a)

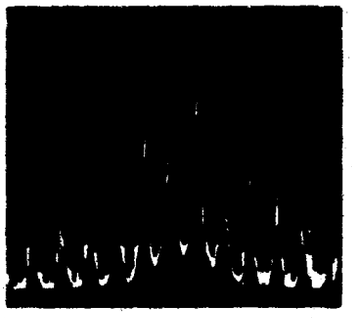

(d) Spectrum of the limiter output signal (Fig. 8(b)) from two equally strong input signals (same as Fig. 7(a))

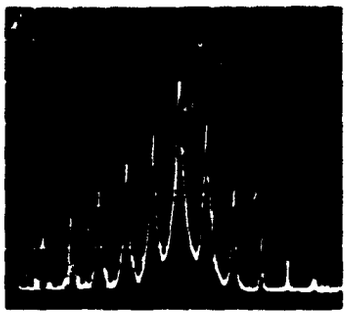

(e) Spectrum of the limiter output signal from two input signals differing by 5 dB (same as Fig. 7(d))

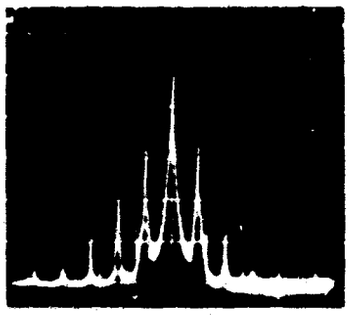

(f) Spectrum of the limiter output signal from two input signals differing by 10 dB (same as Fig. 7(e))

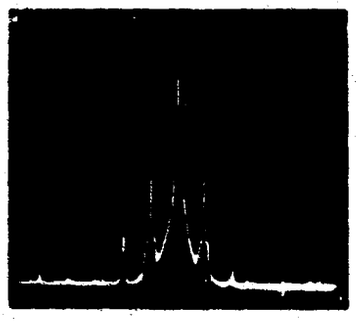

(g) Spectrum of the limiter output signal from two input signals differing by 15 dB (same as Fig. 7(f))

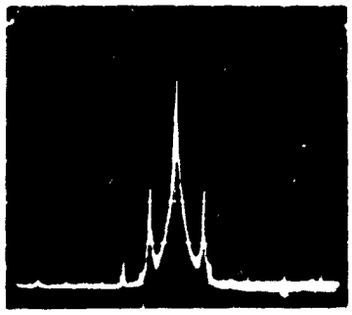

(h) Spectrum of the limiter output signal from two input signals differing by 20 dB (same as Fig. 7(g))

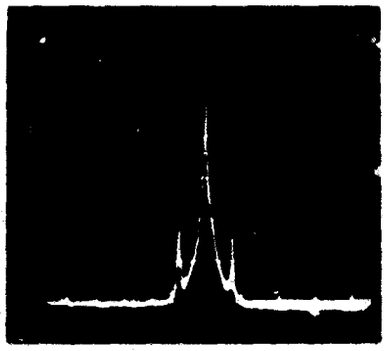

(i) Spectrum of the limiter output signal from two input signals differing by 25 dB (same as Fig. 7(h))

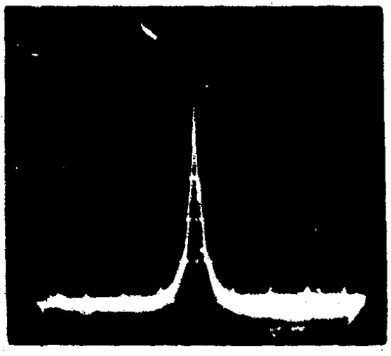

(j) Spectrum of the limiter output signal from one input signal

Fig. 8 - Waveforms and spectra recorded in a bench test

If the input signals differ by as little as 5 dB, the stronger output signal obtains nearly its full size, and the smaller signal appears at approximately -10 dB. That means the smaller signal was suppressed by approximately 5 dB through the limiter and it is accompanied by a slightly smaller image line and by a regularly spaced array of spectral lines which taper off unsymmetrically (Fig. 8(e)). If the input signals differ by 10 dB (Fig. 8(f)), then nearly the full amount of the theoretically predicted 6-dB small signal suppression may be observed. Figures 8(g), 8(h), and 8(i) show the small signal suppressed by 6 dB and accompanied by an equally strong image when the input signals differed by 15, 20, and 25 dB respectively before limiting. Figure 8(j) shows a single spectral line representing the fundamental frequency of a hard-limited single-frequency input. The spectral lines displayed in Figs. 8(d) to 8(i) are the beat frequencies of the two input signals due to the nonlinear processing; the spectral lines are not harmonic frequencies. Harmonic frequencies which are present if a 60-MHz signal is limited would be at multiples of 60 MHz, and they would therefore be outside the spectral range displayed, which covered an interval of approximately 200 kHz centered around 60 MHz.

Point-by-point comparison of the measured spectra such as shown in Fig. 8 and the calculated C_n values pictured in Fig. 7 discloses their exact matching.

This section of the report may be concluded with the remark that the beat frequencies generated through hard limiting would appear like false targets in the case of a CW radar or a pulse doppler radar of insufficient dynamic range. As applied to a pulse doppler radar one may say that two clutter components of slightly different doppler frequencies but both falling in the clutter notch of the processor response — if strong enough to drive the IF amplifier into saturation — may generate beat frequencies which would be within the accepted doppler domain.

It may be noted also that an analogy exists with an antenna problem. False angular responses (ghost targets) are observed in a two-target environment if the elements of an array antenna are nonlinear (7,8).

LIMITING OF A PAIR OF LINEARLY-FREQUENCY-MODULATED SIGNALS

Consider a pair of linearly-frequency-modulated signals in the idealized case where the input signals are entirely overlapping and very strong as compared to thermal noise. The analysis is very similar to the one given in the previous section for the case of constant-frequency sinusoids. A pair of linear FM signals gives rise to beat frequencies within the bandwidth of the frequency excursion. These constitute signals which are compressed by the matched filter or correlator and which will appear, after processing, as an array of false targets both behind and ahead of the pair of true targets (4). If the expanded signals overlap less than completely, there will be a proportionate reduction of the false target magnitudes (4). Let one input signal be given by

$$A_0 \exp j(2\pi f_0 t + bt^2)$$

and the other by a scaled, time- and phase-shifted version of the first signal:

$$A_1 \exp j[2\pi f_0(t - T) + b(t - T)^2 + \phi_{10}] .$$

The instantaneous frequency of the first signal, which is by definition equal to the derivative of its phase divided by 2π, is then equal to

$$f_0 + \frac{b}{\pi} t \ .$$

and the instantaneous frequency of the second signal is given by

$$f_0 + \frac{b}{\pi} (t - T) \ .$$

where T is the mutual time shift between the two input signals. Inserting

$$\phi_0(t) \quad 2\pi f_0 t + bt^2 \tag{24}$$

and

$$\phi_1(t) = 2\pi f_0 (t - T) + b\,(t - T)^2 + \phi_{10} \tag{25}$$

into Eq. (20) results in

$$s_{out}(t) = \sum_{n=-\infty}^{+\infty} C_n \, e^{j[2\pi f_0 (t-nT) + b(t-nT)^2 + n\phi_{10} - (n-1)nbT^2]} \ . \tag{26}$$

Equation (26) says that the limiter output may be decomposed into a summation of linear FM signals. By comparison with the expressions for the input signals one derives that the limiter output consists of an array of mutually-time-shifted images of the input waveforms, with delay T between adjacent components and with amplitude C_n for the nth component.

At the output of the matched filter or correlator which would follow in the signal processing scheme after the hard limiter one would therefore observe an array of compressed pulses, namely, the large signal response with amplitude C_0, the smaller signal response with amplitude C_1, an image response with amplitude C_{-1}, and smaller pulses at regular intervals and with amplitudes C_2, C_3, ... on the side of the smaller true signal and with amplitudes C_{-2}, C_{-3}, ... on the side of the image. If the compressed and detected signals were passed through a logarithmic amplifier, one would be able to observe at its output essentially the same waveforms as the ones depicted in Figs. 8(d) through 8(j). All that has been said in the previous section on the amplitude ratios and capture effects would apply also in the case of linear FM. One could in fact envisage the spectrum analyzer displays 8(d) through 8(j) also as scope pictures for the case of linear FM, simply by considering the traces as functions of time instead of frequency. It is then obvious that one observes false targets in addition to the true targets. This phenomenon may be very cumbersome if the radar should be used for more functions than simple target detection. The way out of this dilemma would of course be to use a receiver and signal processor of sufficiently large dynamic range.

Attention should also be given to the phase term $2\pi f_0 nT$ in Eq. (26), which causes the doppler frequency of false targets to increase with order n if there is a mutual motion between the true targets. This means that the doppler of false targets may be within the acceptance domain of a pulse-compression pulse doppler radar even if the "true" responses due to clutter would be rejected by means of doppler filtering of the compressed signals.

LIMITING OF A PAIR OF ZERO-PI-PHASE-MODULATED SIGNALS

Consider now the class of radar signals which may be generated through switching the phase of a sinusoid between 0 and 180 degrees depending on a binary code. The binary code may be visualized as a sequence of zeros and ones or as a sequence of plus and minus signs or as a video type waveform alternating between two discrete voltage levels. Since the result of this section will be generally valid for any binary coded sequence, no further restriction will be made at this point as to specific code classes. An expression shall be derived for the small and the large signal size after hard limiting as a function of the RF phase ϕ_{10} between the input sinusoids and with the input amplitude ratio a as a parameter. As before in this report the RF signals are assumed to be completely overlapping and strong as compared to the noise. Equation (20) will permit one to decompose the limiter output into a meaningful sum of component signals which may be identified with the input signals. Let the code be represented by a sequence of coefficients c_k whose values are either 0 or 1. The phase modulation impressed on a radar signal may then be expressed as

$$\phi_c(t) = \pi \sum_k c_k \operatorname{rect} \frac{t - k\tau}{\tau} , \tag{27}$$

where the summation runs over all k values, t is the time, τ is the duration of a bit, and rect x stands for Woodward's rectangular function notation:

$$\begin{aligned} \operatorname{rect} x &= 1 , \quad \text{for } x \text{ in the interval } (-0.5, 0.5) , \\ &= 0 , \quad \text{outside the same interval} . \end{aligned} \tag{28}$$

If the carrier frequency is given by f_0, then the phase of the stronger input signal may be written as

$$\phi_0(t) = 2\pi f_0 t + \phi_c(t) , \tag{29}$$

and the phase of the smaller signal may be derived from the phase of the stronger signal through introduction of a time delay T and the mutual RF phase ϕ_{10}:

$$\phi_1(t) = 2\pi f_0 t + \phi_c(t - T) + \phi_{10} . \tag{30}$$

Inserting these expressions into Eq. (20) yields

$$s_{out}(t) = \sum_{n=-\infty}^{+\infty} C_n \, e^{j[n\phi_c(t-T) - (n-1)\phi_c(t) + n\phi_{10}]} \, e^{j2\pi f_0 t} . \tag{31}$$

It is now important to observe that both $\phi_c(t)$ and $\phi_c(t - T)$ can assume only either one of the discrete values 0 or π. Hence

$$\begin{aligned} e^{j[n\phi_c(t-T) - (n-1)\phi_c(t)]} &= e^{j\phi_c(t)} , \quad \text{for all even values of } n , \\ &= e^{j\phi_c(t-T)} , \quad \text{for all odd values of } n . \end{aligned} \tag{32}$$

Equation (31) may therefore be transformed into two separate summations, one of them combining all even-index terms and the other collecting all odd-index terms:

$$s_{out}(t) = \left(\sum_{n=-\infty}^{+\infty} C_{2n}\, e^{j2n\phi_{10}} \right) e^{j\phi_c(t)}\, e^{j2\pi f_0 t}$$

$$+ \left(\sum_{n=-\infty}^{+\infty} C_{2n+1}\, e^{j(2n+1)\phi_{10}} \right) e^{j\phi_c(t-T)}\, e^{j2\pi f_0 t} \quad . \tag{33}$$

From this expression one can read that the limiter output may be written as the summation of two signals, each of them being of the same functional shape as one of the input signals, and with the complex amplitudes described by the sums of exponentially weighted Fourier coefficients of even or odd order respectively:

$$\left(\sum C_{2n}\, e^{j2n\phi_{10}} \right) \quad \text{or} \quad \left(\sum C_{2n+1}\, e^{j(2n+1)\phi_{10}} \right) \quad . \tag{34}$$

These expressions are consequently properly called the amplitude of the stronger signal and the amplitude of the smaller signal after limiting has taken place. Since Eq. (33) is a complete description of the limiter output signal as long as the assumptions made are valid, there is no indication of false targets.

It is possible to transform expressions (34) back to their original domain in a general fashion so that explicit knowledge of Fourier coefficients $C_n(a)$ will not be required for numerical evaluation of capture effects. From Eq. (8) one may derive

$$e^{ja(\theta+\pi)} = \sum C_n(a)\, e^{jn(\theta+\pi)} = \sum (-1)^n\, C_n(a)\, e^{jn\theta} \quad . \tag{35}$$

Hence one obtains through addition of Eqs. (35) and (8)

$$e^{ja(\theta)} + e^{ja(\theta+\pi)} = 2 \sum C_{2n}(a)\, e^{j2n\theta} \quad . \tag{36}$$

Through subtraction one obtains

$$e^{ja(\theta)} - e^{ja(\theta+\pi)} = 2 \sum C_{2n+1}(a)\, e^{j(2n+1)\theta} \quad . \tag{37}$$

These are general relations exactly of the form as needed to express the limiter output signal amplitudes (34) in terms of the function $\exp ja(\theta)$. The large signal amplitude after limiting is

$$\sum C_{2n}\, e^{j2n\phi_{10}} = \left[e^{ja(\phi_{10})} + e^{ja(\phi_{10}+\pi)} \right] / 2 \tag{38}$$

and the small signal amplitude is

$$\sum C_{2n+1}\, e^{j(2n+1)\phi_{10}} = \left[e^{ja(\phi_{10})} - e^{ja(\phi_{10}+\pi)} \right] / 2 \quad . \tag{39}$$

Equations (38) and (39) have been programmed for automatic computer evaluation. The results are depicted in Fig. 9 both for the large and for the small signal distributions. There is a horizontal line at the -3-dB level labeled with the parameter 0 dB indicating that the power is equally split between the output signals if the input signals are equally strong. All curves below or above the -3-dB line refer to the smaller or stronger signal

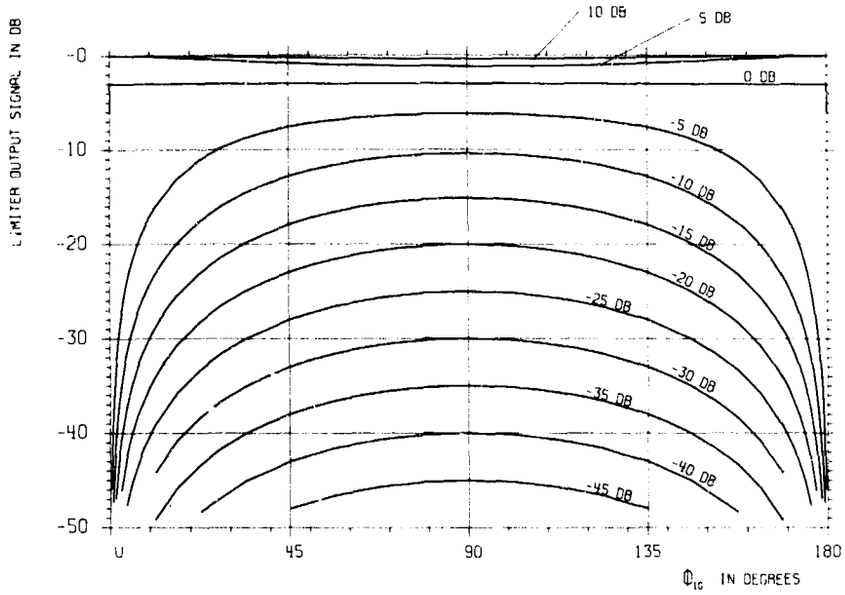

Fig. 9 - Capture of a pair of zero-pi phase-coded signals as a function of the carrier rf phase, with the signal intensity ratio as the parameter

respectively. The curves indicate that the capture effects are minimized if the RF phase between the input signals is around 90 or 270 degrees. If the RF phase amounts to zero or 180 degrees, the smaller signal will be suppressed entirely, at least in the absence of noise or any other type of third signal component. Noise in addition to the two input signals will permit the smaller signal to determine the limiter output signal with some finite probability even in the case of an RF phase difference of 0 or 180 degrees. If there is a correlated third signal at the limiter input, there may be a false target generation effect, as will be shown in the next section. It should be mentioned that Eqs. (38) and (39) may be used to derive a simple geometric construction method in a complex plane to describe the capture effects of two zero-pi-phase-coded signals. It is worth underscoring that Eqs. (38) and (39) properly describe the capture effects no matter what particular binary phase code is used.

GENERAL THEORY OF THE HARD LIMITING OF THREE INPUT SIGNALS

The previous sections have discussed and provided mathematical descriptions of how the limiting of a pair of linear FM signals gives rise not only to capture effects but also to spurious target generation, whereas any kind of zero-pi-phase-coded signal pair is subject only to capture and not to false target generation. The absence of false targets in the case of zero-pi phase codes, although in agreement with general knowledge on this subject, may seem somewhat baffling from a theoretical point of view, in particular since certain pseudo-random sequences, namely linear maximal sequences, which are frequently used as radar modulation functions and which are easily generated by means of feedback shift registers, exhibit a very strong structure and have the property to produce a sequence of the same code but with a different delay if combined linearly. This property justifies the adjective "linear" in "linear maximal sequences," and when one speaks here of a linear code combination, one means the new code generated if two codes with a

relative delay between them are combined according to the rules of Boolean algebra on a bit-to-bit basis. This kind of linear combination would also take place if two phase modulated RF signals are multiplied or beat together, since the multiplication of complex signals results in the addition of the exponents. The effect of signal multiplication takes place at any nonlinear element in the signal channel and especially in a limiter. It was therefore speculated that false targets might be generated, if not in the case of two input signals, in the case of three or more input signals.

The theory developed is a simple extension of the analysis made for the two-input-signal case presented earlier in this report. The same assumptions are made throughout, namely, complete expanded signal overlap and high signal-to-noise ratio. The input signal to the limiter may then be written as

$$\begin{aligned} s_{in} &= A_0\, e^{j\phi_0(t)} + A_1\, e^{j\phi_1(t)} + A_2\, e^{j\phi_2(t)} \\ &= A_0\, e^{j\phi_0(t)}\left(1 + a_1\, e^{j\phi_1} + a_2\, e^{j\phi_2}\right) \\ &= A_0\, e^{j\phi_0(t)}\, R\, e^{j\alpha(t)} . \end{aligned} \tag{40}$$

The convention is that the first signal, $A_0\, e^{j\phi_0(t)}$, is the strongest signal, so that it is meaningful to describe the input signal s_{in} as the strongest signal modified in amplitude and in phase through the presence of two smaller signals, mathematically expressed in Eq. (40) through R and α. Set

$$a_1 = \frac{A_1}{A_0} \quad \text{and} \quad a_2 = \frac{A_2}{A_0} , \tag{41}$$

a_1 and a_2 being the two ratios of a smaller signal to the large signal, and set

$$\theta_1 = \phi_1 - \phi_0 \quad \text{and} \quad \theta_2 = \phi_2 - \phi_0 . \tag{42}$$

The ideal limiter normalizes the amplitude of the input signal, Eq. (40), while preserving its phase function $\phi_0(t) + \alpha(t)$:

$$s_{out} = e^{j[\phi_0(t)+\alpha(t)]} , \tag{43}$$

where α is the phase angle of the complex factor between large parentheses on the second line of Eq. (40):

$$\alpha(t) = \tan^{-1} \frac{a_1 \sin\theta_1 + a_2 \sin\theta_2}{1 + a_1 \cos\theta_1 + a_2 \cos\theta_2} . \tag{44}$$

To obtain a physically meaningful interpretation of the limiter output signal it has to be decomposed into a summation of signals. In the previously treated case of a pair of input signals it proved successful to develop α as a function of θ into a Fourier series. Applying the same technique in the case of a triplet of input signals leads us to consider the development

$$e^{j\alpha(\theta_1,\theta_2)} = \sum_{m=-\infty}^{+\infty} \sum_{n=-\infty}^{+\infty} C_{mn}(a_1, a_2)\, e^{j(m\theta_1 + n\theta_2)} , \tag{45}$$

which is a double Fourier series for α as a function of θ_1 and θ_2. Combining Eq. (43) with Eqs. (45) and (42) leads to the series development for the limiter output:

$$s_{out} = \sum\sum C_{mn}(a_1, a_2)\, e^{j[m\phi_1 + n\phi_2 + (1-m-n)\phi_0]} . \tag{46}$$

The Fourier coefficients C_{mn} may be expressed as a double integral, and they may be determined by numerical integration methods. In the case of practical importance which will be studied in the next section one obtains general expressions for limiter output signal amplitudes which may be transformed back to the original domain, so that any explicit knowledge of Fourier coefficients will not be required. The Fourier series approach permits one to derive relationships in terms of the original quantities.

LIMITING OF A TRIPLET OF LINEAR CODED SEQUENCES

In the case of a triplet of linear coded sequences let the phase modulation function of the strongest signal be given by

$$\phi_c(t) = \mathrm{rep}_{L\tau}\, \pi \sum_{k=1}^{L} c_k \,\mathrm{rect}\, \frac{t - k\tau}{\tau} . \tag{47}$$

where t is the time, τ is the duration of a bit, $c_k = 0$ or 1 depending on a maximal linear sequence, L is the code length, and $\mathrm{rep}_{L\tau}$ indicates the periodic repetition of the code, the repetition period being equal to $L\tau$. A modulation function of this kind is usually generated by means of shift registers with suitable feedback connections. A shift register generator consisting of S stages may be used to generate a code of length $L = 2^S - 1$. This kind of code generation is frequently used in radar, both for theoretical and practical reasons. This method requires little hardware, and it yields a code with a nearly ideal autocorrelation function, the range side lobes being at a uniform level of $-20 \log L$ dB below the main peak. The low and uniform-range side-lobe level is a consequence of the strong structure inherent in this kind of pseudo-random sequence, namely, of the property that the codes added bit by bit to a delayed version of the same code under the rules of Boolean algebra will result in the original code sequence shifted by a pseudo-random number of bits. It will be seen that the same property is responsible for the generation of a false target of sometimes larger magnitude than any one of the suppressed true target returns.

As an example consider the shift register generator depicted in Fig. 10. At its output one would observe a periodic binary code sequence, the repetition period being equal to 31 clock pulse intervals. Since the shift register contains five stages, the feedback is connected as shown in Fig. 10 to ensure maximum code length and $L = 2^S - 1 = 2^5 - 1 = 31$. If one would start to count a new period for example when the shift register is loaded with the sequence 1, 0, 0, 0, 0, then as a consequence of the operation depicted in the figure one would be able to record the output

1000010101110110001111100110100.

If this code word is added to the same word but shifted to the right by one bit, namely,

0100001010111011000111110011010,

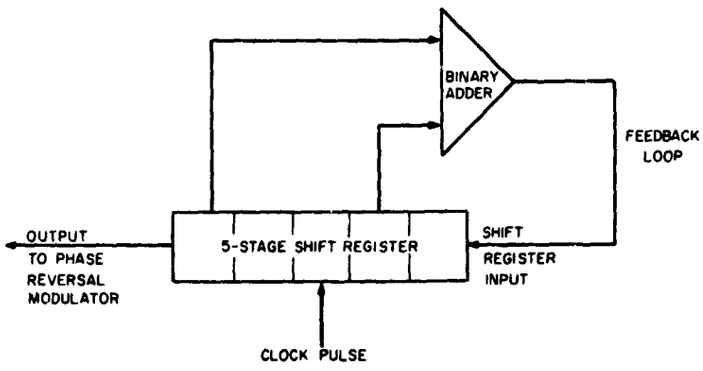

Fig. 10 - Maximum-code-length shift register code generator

one obtains as a result of the binary addition the new code word

$$1100011111001101001000010101110.$$

The remarkable feature of linear coded sequences is that the code word obtained is not any arbitrary sequence but is the same as the original sequence shifted by a number of bits, in this case shifted by 18 bits as one can easily verify by inspection of the sequences. Binary code addition takes place if a signal of the type $\exp j\phi_c(t)$ is multiplied with another signal $\exp j\phi_c(t-T)$, T being the relative delay between the two signals, since the product of $\exp j\phi_c(t)$ and $\exp j\phi_c(t-T)$ is $\exp j[\phi_c(t) + \phi_c(t-T)]$. In the special case of linear coded sequences one has then

$$e^{j\phi_c(t)}\, e^{j\phi_c(t-T)} = e^{j\phi_c(t-T')}$$

and also

$$e^{j\phi_c(t)}\, e^{j\phi_c(t-T_1)}\, e^{j\phi_c(t-T_2)} = e^{j\phi_c(t-T')} \quad (48)$$

T' being a delay which depends in a pseudo-random fashion on the shift between the codes added together.

Now apply the results from the previous section. The limiter input signal is mathematically described by Eq. (40), where the exponent of the strongest signal is

$$j\phi_0(t) = j[\phi_c(t) + 2\pi f_0 t]\ , \quad (49)$$

the exponent of the second signal is

$$j\phi_1(t) = j[\phi_c(t-T_1) + 2\pi f_0 t + \phi_{10}]\ , \quad (50)$$

and the exponent of the third signal is

$$j\phi_2(t) = j[\phi_c(t-T_2) + 2\pi f_0 t + \phi_{20}]\ . \quad (51)$$

Here, f_0 is the RF frequency, ϕ_{10} and ϕ_{20} are the RF phases between the second and the first and the third and the first signal respectively, and T_1 and T_2 are the mutual delays. Inserting Eqs. (49), (50), and (51) into Eq. (46) results in

$$s_{out} = \sum\sum C_{mn}(a_1, a_2)\, e^{j(m\phi_{10} + n\phi_{20})} \times e^{-j(m+n-1)\phi_c(t) + jm\phi_c(t-T_1) + jn\phi_c(t-T_2)}\, e^{j2\pi f_0(t)} \tag{52}$$

This expression may be significantly simplified if one realizes that $\exp jk\phi_c$ is equal to $\exp j\phi_c$ or to 1, depending on whether k is odd or even. Using also the property given by Eq. (48) one can write the following truth table for the exponential expression $\exp\,[-j(m+n-1)\phi_c(t) + jm\phi_c(t-T_1) + jn\phi_c(t-T_2)]$:

	even m	odd m
even n	$e^{j\phi_c(t)}$	$e^{j\phi_c(t-T_1)}$
odd n	$e^{j\phi_c(t-T_2)}$	$e^{j[\phi_c(t)+\phi_c(t-T_1)+\phi_c(t-T_2)]}$ $e^{j\phi_c(t-T')}$

One can now write Eq. (52) in the form of a sum of four terms in such a way that each index of a Fourier coefficient C_{mn} is even or odd throughout each summation:

$$\begin{aligned} s_{out} = {} & \left[\sum_k \sum_\ell C_{2k,2\ell}(a_1, a_2)\, e^{j(2k\phi_{10} + 2\ell\phi_{20})}\right] e^{j\phi_c(t)}\, e^{j2\pi f_0 t} \\ & + \left\{\sum_k \sum_\ell C_{2k+1,2\ell}(a_1, a_2)\, e^{j[(2k+1)\phi_{10} + 2\ell\phi_{20}]}\right\} e^{j\phi_c(t-T_1)}\, e^{j2\pi f_0 t} \\ & + \left\{\sum_k \sum_\ell C_{2k,2\ell+1}(a_1, a_2)\, e^{j[2k\phi_{10} + (2\ell+1)\phi_{20}]}\right\} e^{j\phi_c(t-T_2)}\, e^{j2\pi f_0 t} \\ & + \left\{\sum_k \sum_\ell C_{2k+1,2\ell+1}(a_1, a_2)\, e^{j[(2k+1)\phi_{10} + (2\ell+1)\phi_{20}]}\right\} e^{j\phi_c(t-T')}\, e^{j2\pi f_0 t} \end{aligned} \tag{53}$$

This expression shows that the limiter output consists of four signals, three of them being identical with the three input signals except for an amplitude change and the fourth signal being an image of the coded sequence at some pseudo-random starting position. The amplitudes of all four signals can be calculated if the ratios of the small to large signals before limiting and the RF phases are known, without requiring specification of the particular linear code used. The amplitudes are given by the expressions in the large enclosures in Eq. (53). These are also the amplitudes which the four correlation peaks of the signal s_{out} will have after crosscorrelation processing with respect to the transmitted radar code $\phi_1(t)$. It is hence possible to derive quantitative information about capture and false target generation effects by evaluating the sums of Fourier coefficients as indicated by Eq. (53).

As has been indicated, the Fourier series approach reveals its usefulness and power through the fact that the summations in Eq. (53) can be transformed back to the original domain, thereby enabling numerical discussion of results without a need to know the Fourier coefficients. Through inserting the arguments $a_1 + \pi$ and/or $a_2 + \pi$ in place of a_1 and/or a_2 in Eq. (45), one derives the following three relations:

$$e^{j\alpha(\theta_1+\pi,\theta_2)} = \sum_m \sum_n (-1)^m C_{mn}(a_1, a_2)\, e^{j(m\theta_1+n\theta_2)}, \tag{54}$$

$$e^{j\alpha(\theta_1,\theta_2+\pi)} = \sum_m \sum_n (-1)^n C_{mn}(a_1, a_2)\, e^{j(m\theta_1+n\theta_2)}, \tag{55}$$

and

$$e^{j\alpha(\theta_1+\pi,\theta_2+\pi)} = \sum_m \sum_n (-1)^{m+n} C_{mn}(a_1, a_2)\, e^{j(m\theta_1+n\theta_2)}. \tag{56}$$

These expressions contain the same Fourier components as Eq. (45), however, with alternating signs, so that coefficients with even or odd m and n values may be made to reinforce or cancel by suitably combining Eqs. (45), (54), (55), and (56). Thereby a back transform for the amplitude relations in Eq. (53) is obtained.

In adding Eq. (45) and Eq. (54) all the terms with even m values will be doubled and all the terms with odd m values will be canceled. This may be written in the following self-explanatory shorthand notation:

$$(45) + (54) = 2 \sum_{\substack{\text{all} \\ \text{even} \\ m\text{'s}}} \sum_{\substack{\text{all} \\ n\text{'s}}} C \ldots . \tag{57}$$

In a similar fashion one obtains three more useful linear combinations:

$$(45) - (54) = 2 \sum_{\substack{\text{all} \\ \text{odd} \\ m\text{'s}}} \sum_{\substack{\text{all} \\ n\text{'s}}} C \ldots , \tag{58}$$

$$(55) + (56) = 2 \sum_{\substack{\text{all} \\ \text{even} \\ m\text{'s}}} \sum_{\substack{\text{all} \\ n\text{'s}}} (-1)^n C \ldots . \tag{59}$$

and

$$(55) - (56) = 2 \sum_{\substack{\text{all} \\ \text{odd} \\ m\text{'s}}} \sum_{\substack{\text{all} \\ n\text{'s}}} (-1)^n C \ldots . \tag{60}$$

Now linear combinations are formed between Eqs. (57) and (59) or between Eqs. (58) and (60) with the purpose of reinforcing or canceling terms with even or odd n's. One obtains four linear combinations of interest:

$$(57) + (59) = (45) + (54) + (55) + (56)$$

$$= 4 \sum_{\substack{\text{all} \\ \text{even} \\ m\text{'s}}} \sum_{\substack{\text{all} \\ \text{even} \\ n\text{'s}}} C \ldots . \tag{61}$$

$$(58) + (60) = (45) - (54) + (55) - (56)$$

$$= 4 \sum_{\substack{\text{all} \\ \text{odd} \\ n\text{'s}}} \sum_{\substack{\text{all} \\ \text{even} \\ n\text{'s}}} C \ldots , \tag{62}$$

$$(57) - (59) = (45) + (54) - (55) - (56)$$

$$= 4 \sum_{\substack{\text{all} \\ \text{even} \\ n\text{'s}}} \sum_{\substack{\text{all} \\ \text{odd} \\ n\text{'s}}} C \ldots , \tag{63}$$

and

$$(58) - (60) = (45) - (54) - (55) + (56)$$

$$= 4 \sum_{\substack{\text{all} \\ \text{odd} \\ n\text{'s}}} \sum_{\substack{\text{all} \\ \text{odd} \\ n\text{'s}}} C \ldots . \tag{64}$$

These linear combinations are expressions exactly of the form needed to express the amplitudes in Eq. (53) in terms of $e^{j\alpha}$.

From Eq. (61) one obtains the amplitude of target 1 (strongest target):

Target 1 amplitude = 0.25

$$\left[e^{j\alpha(\phi_{10}-\phi_{10})} + e^{j\alpha(\phi_{10}+\pi-\phi_{20})} + e^{j\alpha(\phi_{10}-\phi_{20}+\pi)} + e^{j\alpha(\phi_{10}+\pi-\phi_{20}+\pi)}\right] . \tag{65}$$

From Eq. (62) one obtains the amplitudes of the second-strongest true target:

Target 2 amplitude = 0.25

$$\left[e^{j\alpha(\phi_{10}-\phi_{20})} - e^{j\alpha(\phi_{10}+\pi-\phi_{20})} + e^{j\alpha(\phi_{10}-\phi_{20}+\pi)} - e^{j\alpha(\phi_{10}+\pi-\phi_{20}+\pi)}\right] . \tag{66}$$

The smallest true target amplitude is obtained from Eq. (63):

Target 3 amplitude = 0.25

$$\left[e^{j\alpha(\phi_{10}-\phi_{20})} + e^{j\alpha(\phi_{10}+\pi-\phi_{20})} - e^{j\alpha(\phi_{10}-\phi_{20}+\pi)} - e^{j\alpha(\phi_{10}+\pi-\phi_{20}+\pi)}\right] . \tag{67}$$

The false target amplitude follows from Eq. (64):

False target amplitude = 0.25

$$\left[e^{j\alpha(\phi_{10}-\phi_{20})} - e^{j\alpha(\phi_{10}+\pi-\phi_{20})} - e^{j\alpha(\phi_{10}-\phi_{20}+\pi)} + e^{j\alpha(\phi_{10}+\pi-\phi_{20}+\pi)}\right] . \tag{68}$$

Equations (65) through (68) are complex notations describing both the amplitude change, i.e., capture effect, and the phase change due to limiting. A problem exists how to present the amplitude distributions which depend on two variables (ϕ_{10} and ϕ_{20}) and on two

parameters (a_1 and a_2). It was decided to write a program for the NRL CDC-3800 computer, using separate real and imaginary expressions for $\exp j\alpha(\theta_1,\theta_2)$ derived from Eq. (44):

$$Re\ e^{j\alpha(\theta_1,\theta_2)} = \frac{1 + a_1 \cos\theta_1 + a_2 \cos\theta_2}{\sqrt{(1 + a_1 \cos\theta_1 + a_2 \cos\theta_2)^2 + (a_1 \sin\theta_1 + a_2 \sin\theta_2)^2}}. \tag{69}$$

and

$$Im\ e^{j\alpha(\theta_1,\theta_2)} = \frac{a_1 \sin\theta_1 + a_2 \sin\theta_2}{\sqrt{(1 + a_1 \cos\theta_1 + a_2 \cos\theta_2)^2 + (a_1 \sin\theta_1 + a_2 \sin\theta_2)^2}}. \tag{70}$$

The product obtained from the computer is a punched paper tape which contains the data for a pseudo-three-dimensional plot to be drawn by the Gerber plotting machine at NRL. Thus any handling of numerical data by a draftsman is circumvented.

This report shows the resulting absolute value amplitude distributions for three cases: Figs. 11 are for three equally strong signals at the limiter input; Figs. 12 are for two equally strong signals at the limiter input, with the third signal 10 dB smaller than either one of the stronger signals; and Figs. 13 are for one strong signal and two smaller signals, each of which is at a -10-dB level with respect to the strongest signal. The strongest false target is observed if the three true target signals are equally strong and in phase or 180 degrees out of phase. In this case each of the true target waveforms and the false target will appear with an amplitude equal to 1/2 of the maximum possible amplitude. With finite length codes the false target may actually be slightly stronger than any one of the true targets. This effect is due to the interference of range side lobes, as will be explained shortly.

If one has two equally strong signals and one smaller signal at the limiter input, then a false target is generated of approximately the same size as the captured smaller signal, as can be seen from comparing the surface in Fig. 12(d) with the surface in Fig. 12(c). The two stronger signals suffer capture to an extent depending on their relative phasing, and it should be noted (Figs. 12(a) and 12(b)) that each maximum of one signal coincides with a minimum of the other signal component.

It has been discussed that there is no false target generation effect if there are only two signals at the limiter input. It should therefore be no surprise that the false target size is much reduced if two of the three true target signals are relatively small (Fig. 13(d)). The discussion of capture and effects of false target generation is much simplified if all input signals are equally strong and if their mutual RF phases are equal to 0 or 180 degrees. Then one can read from Eq. (44) or from Eqs. (69) and (70) that $\exp j\alpha(\theta_1,\theta_2) = 1$ if at least one of the arguments is equal to 0 and that $\exp j\alpha(\pi,\pi) = -1$. To obtain the captured target and the false target amplitudes, one has to combine the exponential functions according to Eqs. (65) through (68). One obtains the following:

Case 1: All true targets having the same polarity, i.e., $\phi_{10} = \phi_{20} = 0$:

$$\text{target 1 amplitude} = 0.25\,[(1) + (1) + (1) + (-1)] = 0.5$$

$$\text{target 2 amplitude} = 0.25\,[(1) - (1) + (1) - (-1)] = 0.5$$

$$\text{target 3 amplitude} = 0.25\,[(1) + (1) - (1) - (-1)] = 0.5$$

$$\text{false target amplitude} = 0.25\,[(1) - (1) - (1) + (-1)] = -0.5.$$

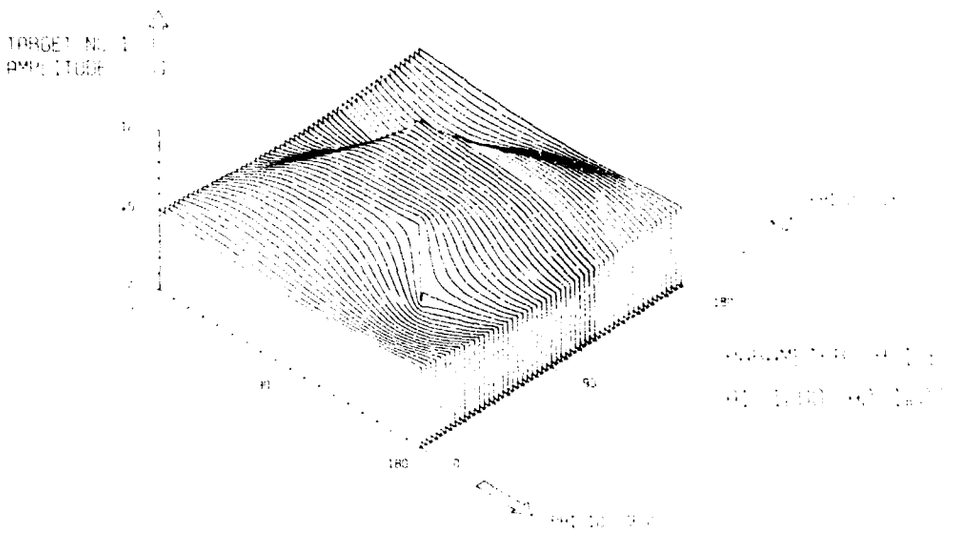

Fig. 11(a) - True target 1 amplitude for the case of three equally strong expanded signals using zero-pi shift register phase coding (for machine convenience the parameters ϕ_{10}, ϕ_{20}, a_1, and a_2 are labeled as shown)

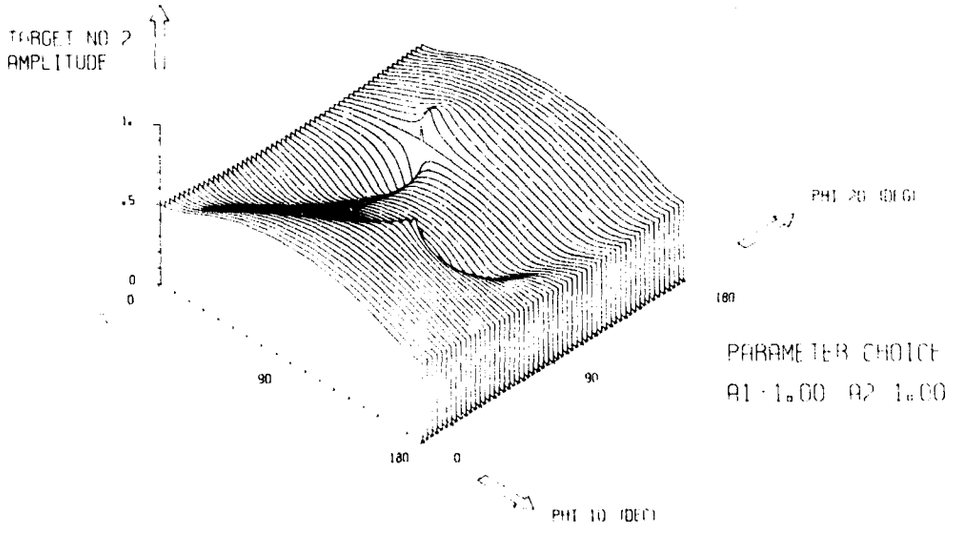

Fig. 11(b) - True target 2 amplitude for the case of three equally strong expanded signals using zero-pi shift register phase coding

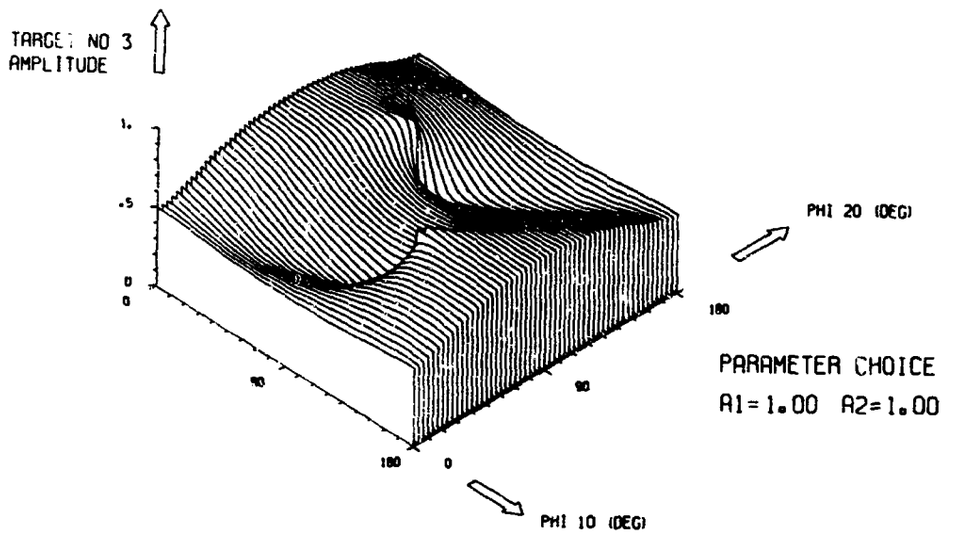

Fig. 11(c) - True target 3 amplitude for the case of three equally strong expanded signals using zero-pi shift register phase coding

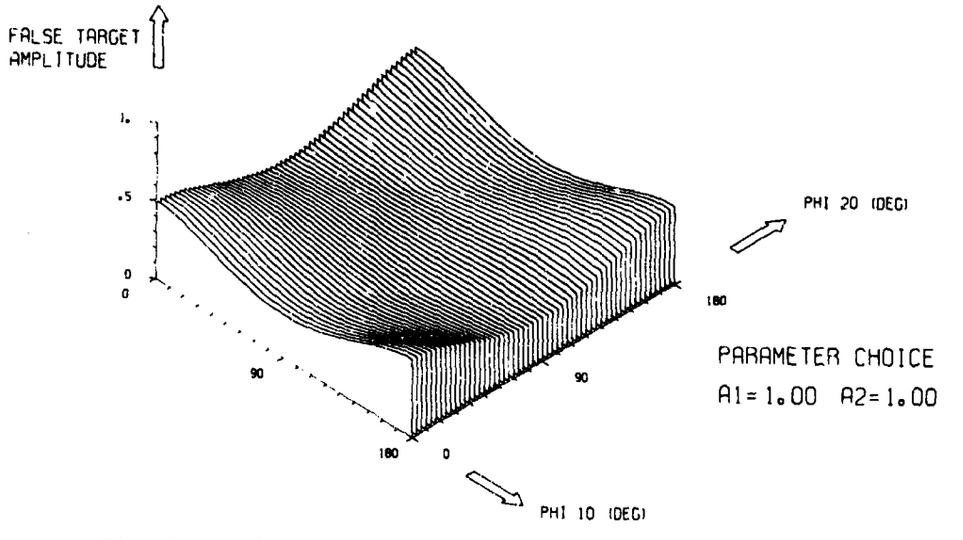

Fig. 11(d) - False target amplitude for the case of three equally strong expanded signals using zero-pi shift register phase coding

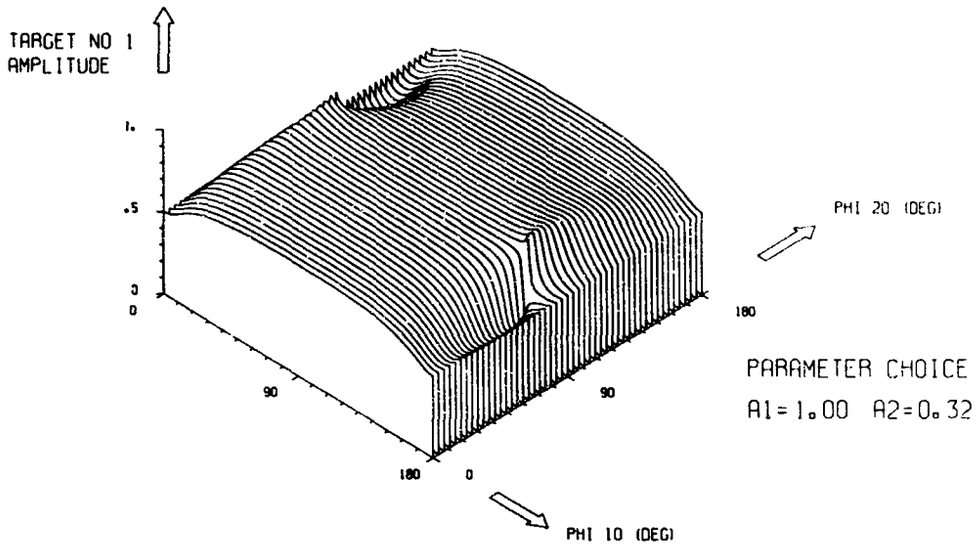

Fig. 12(a) - True target 1 amplitude for the case of two equally strong targets and one smaller true target using zero-pi shift register phase coding

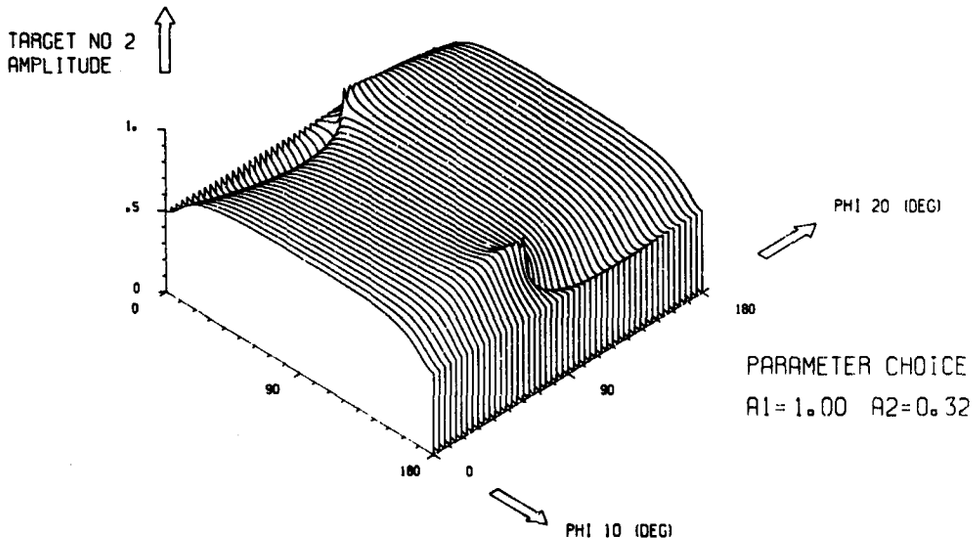

Fig. 12(b) - True target 2 amplitude for the case of two equally strong targets and one smaller true target using zero-pi shift register phase coding

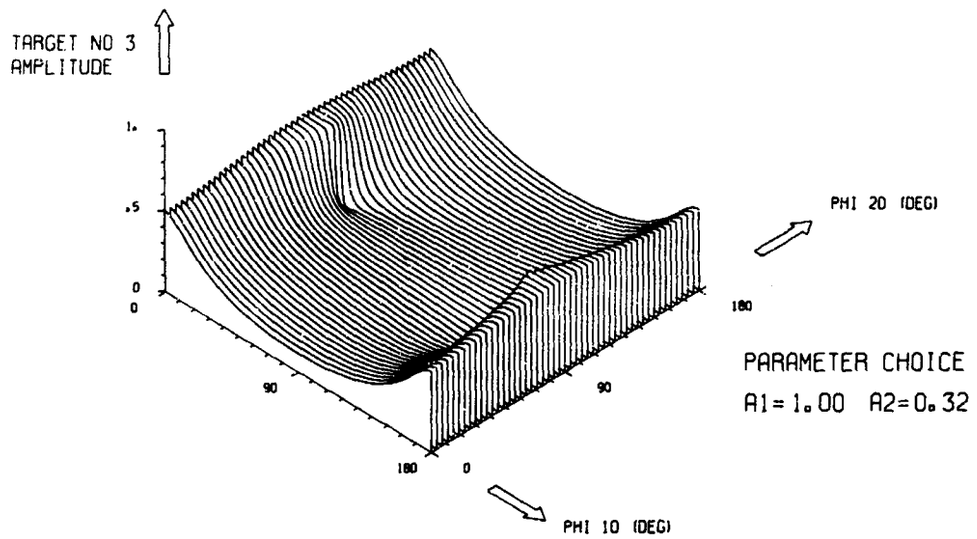

Fig. 12(c) – True target 3 amplitude for the case of two equally strong targets and one smaller true target using zero-pi shift register phase coding

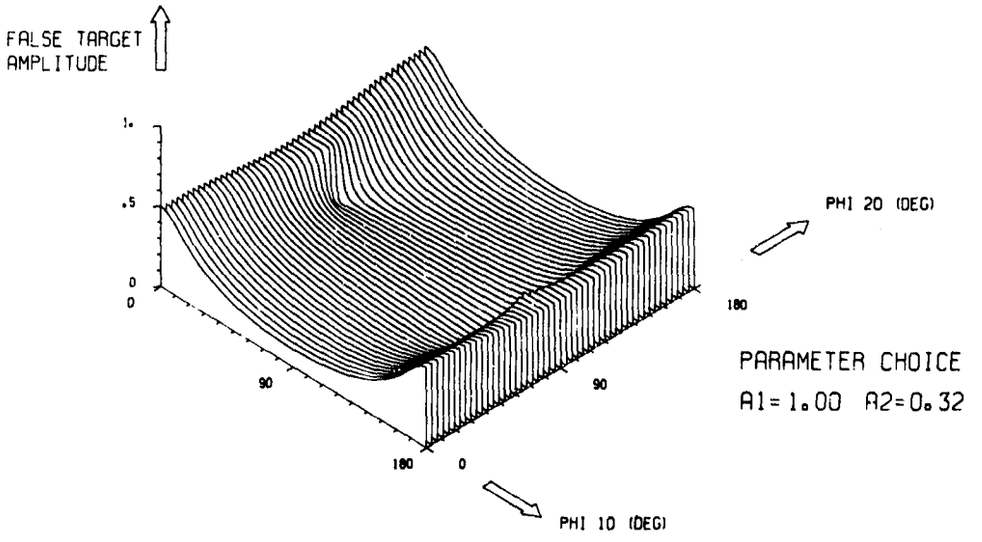

Fig. 12(d) – False target amplitude for the case of two equally strong targets and one smaller true target using zero-pi shift register phase coding

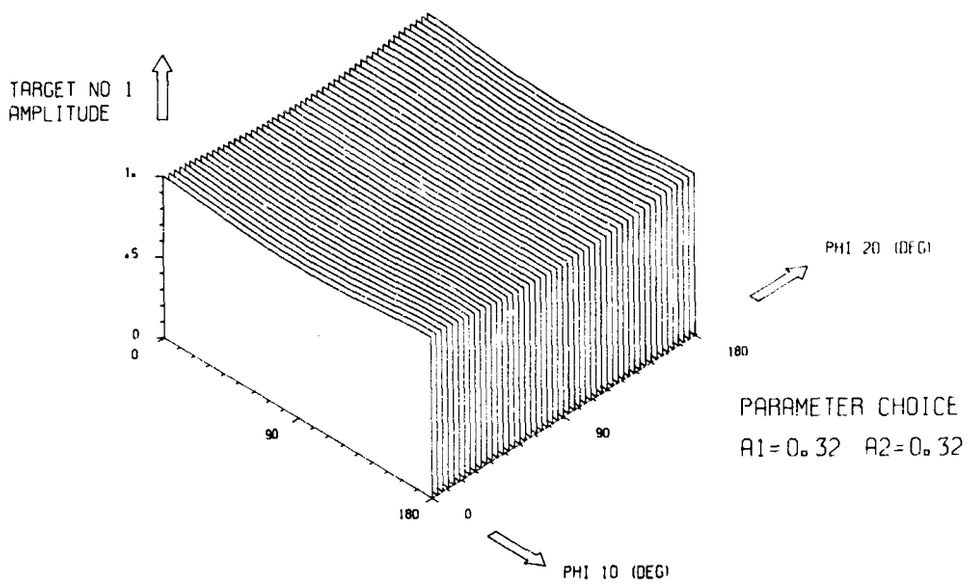

Fig. 13(a) - True target 1 amplitude for the case of one strong target and two equal intensity smaller true targets using zero-pi shift register phase coding

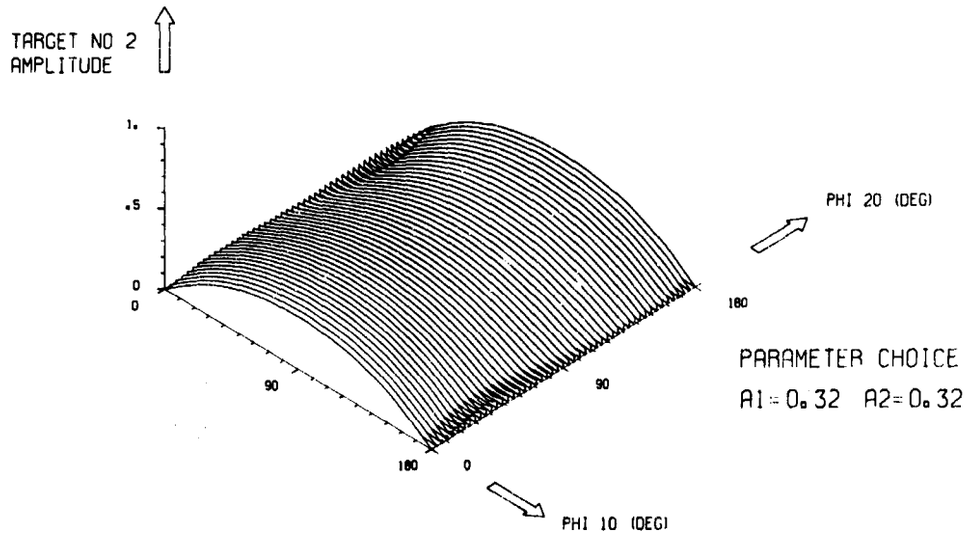

Fig. 13(b) - True target 2 amplitude for the case of one strong target and two equal intensity smaller true targets using zero-pi shift register phase coding

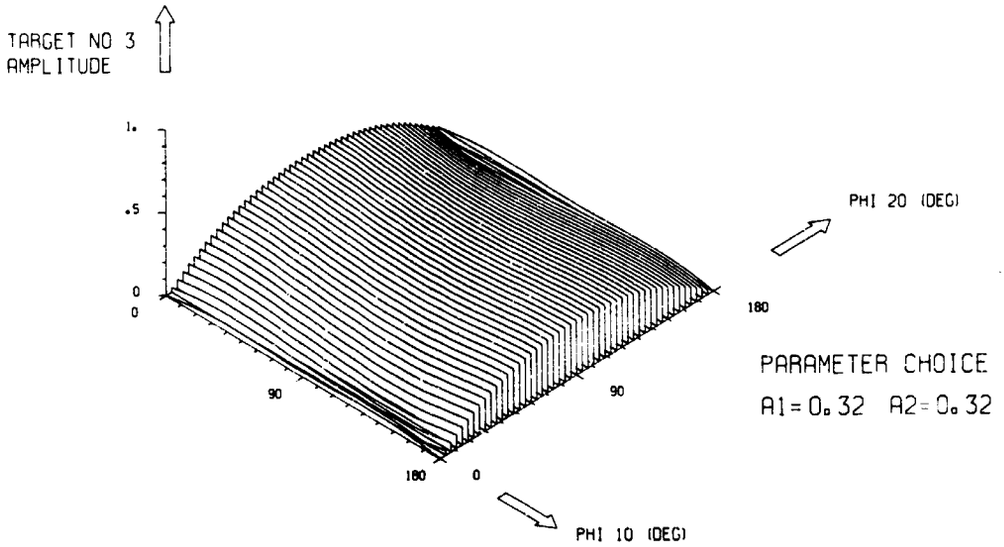

Fig. 13(c) - True target 3 amplitude for the case of one strong target and two equal intensity smaller true targets using zero-pi shift register phase coding

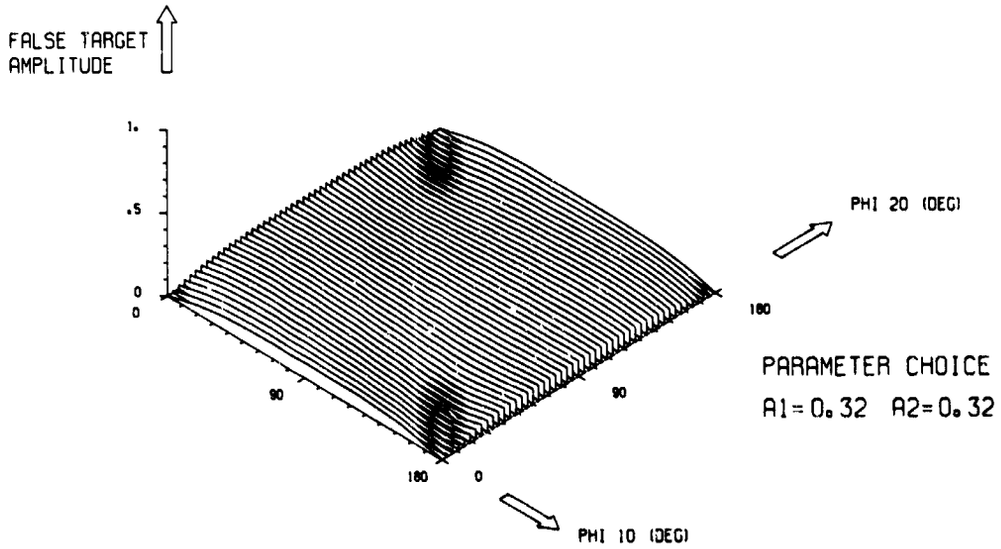

Fig. 13(d) - False target amplitude for the case of one strong target and two equal intensity smaller true targets using zero-pi shift register phase coding

After hard limiting there will be four signals, each of them having 1/2 the maximum possible amplitude, three of the signals corresponding in time shift and polarity to the true input signals and the fourth signal corresponding to a false target with a polarity opposite to the true target polarity.

Case 2: One of the true targets having phase opposition with the remaining pair of true targets, e.g., $\phi_{10} = 0$ and $\phi_{20} = \pi$:

$$\text{target 1 amplitude} = 0.25\,[(1) + (-1) + (1) + (1)] = 0.5$$

$$\text{target 2 amplitude} = 0.25\,[(1) - (-1) + (1) - (1)] = 0.5$$

$$\text{target 3 amplitude} = 0.25\,[(1) + (-1) - (1) - (1)] = -0.5$$

$$\text{false target amplitude} = 0.25\,[(1) - (-1) - (1) + (1)] = 0.5.$$

The limiter output contains again three signals of the same polarity and one signal of the opposite polarity. One of the three same-polarity signals corresponds to a false target, and the opposite polarity signal corresponds to one of the true targets in this case. It should be obvious that the polarity of the compressed signals can consequently not be evaluated to permit discrimination between true and false targets.

Consider the output signal obtained from a matched filter or a pulse compression device. In the single-target case one will obtain an impulse-like point target response, consisting of a central spike of height N, where N is equal to the length of the code, surrounded by uniform-range side lobes at the -1 level. This type of autocorrelation function is depicted in Fig. 14(a). If there are three input signals of equal intensity, corresponding to one of the two previously considered cases, there will be three correlation spikes of one polarity, corresponding to three true targets in case 1 or to two true targets and one false target in case 2, of a magnitude $N/2 - 1$, and one correlation spike with the opposite polarity, corresponding to a false target or a true target and with a magnitude $N/2 + 1$. The addition or subtraction of 1 from $N/2$ originates from the constructive or destructive interference of a uniform-range-side-lobe level with the correlation peaks. Hence it may happen that the false target is larger than any one of the true target responses.

The existence of a spurious target response has been confirmed by a computer simulation. Figure 14(a) shows the autocorrelation function of a maximum-length linear shift register code with $L = 63$ bits. This function is descriptive of the radar response to a single point target. Figure 15(a) is a plot of the processor response due to three equally strong equi-phase true targets. The response is obtained through addition of three mutually delayed binary-coded video signals, hard limiting, and crosscorrelation with the original code. The resulting crosscorrelation function shows a spurious response exactly as predicted by the theory. The preservation of a uniform-range-side-lobe level and the predicted capture effect are confirmed. The uniform-range-side-lobe level is preserved since the crosscorrelation function depicted in Fig. 15(a) is the same as the sum of four autocorrelation functions, each of them having uniform side-lobe levels as shown in Fig. 14(a), weighted with the factors +1/2 or -1/2, and mutually delayed by the amounts T_1, T_2, and T'.

Figure 16(a) when compared with Fig. 15(a) exhibits that the false target may undergo a very erratic motion if the true target geometry changes but very slightly. This erratic motion effect may be used in a video integration process to enhance the ratio of true targets to false targets.

Fig. 14(a) - Simulated radar response to a single target, for a radar using a 63-bit repetitive code

Fig. 14(b) - Simulated radar response to a single target, for a radar using a 63-bit truncated code

Fig. 15(a) - Simulated radar response to three point targets, for a radar using a 63-bit repetitive code

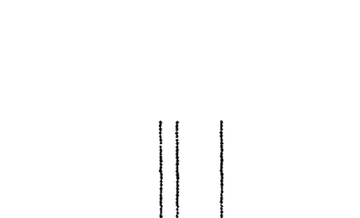

Fig. 15(b) - Simulated radar response to three point targets, for a radar using a 63-bit truncated code

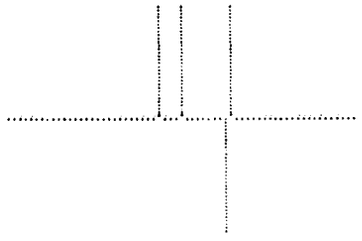

Fig. 16(a) - Simulated radar response to three point targets, of a slightly varied geometry, for a radar using a 63-bit repetitive code

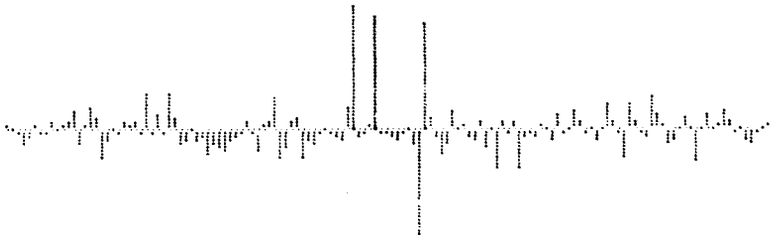

Fig. 16(b) - Simulated radar response to three point targets, of a slightly varied geometry, for a radar using a 63-bit truncated code

Figures 14(b), 15(b), and 16(b) show the pulse compression waveforms obtained if the code sequences are truncated. It is known that truncation increases the average range-side-lobe level. The spurious targets may be observed at the same locations where they would be if the code sequence were repeated. The false target response may be of reduced magnitude and depends on how much the expanded radar signals overlap. Since the range-side-lobe structure of truncated sequences is very complicated and irregular, an exact theory to quantitatively explain capture and false target generation effects should not be expected.

CONCLUSIONS

It is shown in this report that hard limiting of superimposed expanded radar returns may cause a false target effect in addition to the well-known capture effect. The false target effect has been known for the case of a pair of linear FM radar returns. It is shown that a zero-pi-phase-coded radar signal modulated by a maximum-length shift register sequence may be subject to a false target effect. It is interesting to note that with two targets in the case of zero-pi phase coding there is capture only and no false target effect; at least three true targets must be taken into account to show the existence of a false target. This study may serve as an example to show the erroneous conclusions one may reach, in nonlinear systems theory, by deriving rules about multiple target responses from the study of a two-target model.

To avoid false target effects one must avoid the limiting of expanded radar returns having a high signal-to-noise ratio.

ACKNOWLEDGMENTS

Comments from R. J. Adams and S. K. Meads are hereby gratefully acknowledged. The author thanks R. M. Crisler for running a bench test and for making the results available for this report. The author also gratefully acknowledges the encouraging comments of Dr. E. C. Watters, of the Westinghouse Electric Corporation

REFERENCES

1. Ristenbatt, M.P., "Pseudo-Random Binary Coded Waveforms," chapter 4 of "Modern Radar," edited by Raymond S. Berkowitz, Wiley, New York, 1965

2. Manasse, R., Price, R., and Lerner, R.M., "Loss of Signal Detectability in Band-Pass Limiters," IRE Trans. Information Theory IT-4:34-38 (Mar. 1958)

3. Bogotch, S.E., and Cook, C.E., "The Effect of Limiting on the Detectability of Partially Time-Coincident Pulse Compression Signals," IEEE Trans. Mil. Electronics MIL-9:17-24 (Jan. 1965)

4. Nolen, J.C., "Effects of Limiting on Multiple Signals," Proceedings of the Symposium on Recent Advances in Matched Filter Theory and Pulse Compression Techniques, RADC-TR-59-161, Sept. 1959, pp. 295-317

5. Jahnke E., and Emde, F., Tables of Functions, 4th ed., Dover, New York, 1945, chapter VIII

6. Cahn, C.R., "A Note on Signal-to-Noise Ratio in Band-Pass Limiters," IRE Trans. Information Theory IT-7:39-43 (Jan. 1961)

7. Banta, E.D., "Spurious Responses in Linear Arrays Using Nonlinear Elements," IEEE Trans. Antennas Propagation AP-12:129-130 (Jan. 1964)

8. Kovaly, J.J., and Miller, S.N., "A Superlimiting Phased-Array Receiving System in a Two-Source Environment," IEEE Trans. Aerospace Electronic Systems AES-3: 518-526 (May 1967)

Appendix

NUMERICAL DETERMINATION OF THE FOURIER COEFFICIENTS

The coefficients C_n are the Fourier coefficients of the complex function $\exp j\alpha(\theta)$ as can be seen from Eq. (8). The fast Fourier transform is a convenient technique for the given task, in particular since it is "naturally" adapted to the handling of complex variables. Therefore a program has been written in the XTRAN language for a time-sharing computer terminal facility at NRL, using an FFT subroutine provided by Comshare. A program listing is reproduced at the end of this appendix.

The program goes through the following logical steps:

1. Read N = number of samples; this must be a power of 2.

2. Read the small-to-large signal ratio.

3. Compute a period of the function $\exp j\alpha(\theta)$ at the N sampling points

$$\theta_n = \frac{2\pi}{N}(n-1) ,$$

using separate numerical expressions for the real and for the imaginary parts of the function

$$\alpha(\theta) = \rho \tan^{-1}[(1+\sin\theta)/(1+a\cos\theta)]$$

$$\frac{1+a\cos\theta}{\sqrt{1+a^2+2a\cos\theta}} + j\frac{a\sin\theta}{\sqrt{1+a^2+2a\cos\theta}}$$

4. Calculate the Fourier coefficients of this function by means of an FFT subroutine.

5. Print out all C_n values of interest (the printout being restricted to the range n = -15, -14, ..., 14, 15 and C_n > -60 dB).

6. Go to step 1 to reinitiate the program with a new data set. (Subsequent to step 5 the program returns to its starting point so that a new data set can be read and the corresponding C_n values can be determined. The program recycles until its execution is interrupted by an "escape" command to the computer.)

To ensure that a sufficiently large number of sampling points was used, their number was increased by factors of 2 from one iteration to the next until the calculated coefficients remained the same to within 0.01 dB. To exhibit the convergence of the computed C_n values toward a limit when the number of samples is increased, the sequence of printouts for 20 log a = -10 dB and for N = 8, 16, 32, and 128 samples is reproduced within Table A1.

Table A.1
Values Printed Out for 20 log a = -10 dB
and for N = 8, 16, 32, and 128 Samples

Order	C_n	C_n (dB)	Order	C_n	C_n (dB)
Number of Points N = 8			Number of Points N = 32		
-4	0.0022	-53.14	-4	0.0026	-51.67
-3	-0.0094	-40.58	-3	-0.0094	-40.50
-2	0.0359	-28.90	-2	0.0359	-28.90
-1	-0.1521	-16.36	-1	-0.1521	-16.36
0	0.9745	-0.22	0	0.9745	-0.22
1	0.1601	-15.91	1	0.1602	-15.91
2	-0.0126	-37.98	2	-0.0128	-37.84
3	0.0013	-57.72	3	0.0020	-53.80
Number of Points N = 16			Number of Points N = 128		
-4	0.0026	-51.67	-4	0.0026	-51.67
-3	-0.0094	-40.50	-3	-0.0094	-40.50
-2	0.0359	-28.90	-2	0.0359	-28.90
-1	-0.1521	-16.36	-1	-0.1521	-16.36
0	0.9745	-0.22	0	0.9745	-0.22
1	0.1602	-15.91	1	0.1602	-15.91
2	-0.0128	-37.84	2	-0.0128	-37.84
3	0.0020	-53.80	3	0.0020	-53.80

In this case 16 data points are sufficient. The printouts remain the same for a larger number of data points, as shown for N = 32 and 128. The use of only eight data points would entail some error, especially as far as the relatively smaller size beat products are concerned.

The largest number of samples was required in the vicinity of a = 1, i.e., if $g(\theta)$ was close to a linear sawtooth function. In this case a 1024-point transform was selected. For smaller a values a much smaller number of sampling points sufficed.

The validity of the program was checked by the following criteria:

1. The imaginary part of the Fourier coefficients turned out to be 0 within the confines of roundoff errors, as required by the theory presented in the section "General Theory of the Hard Limiting of Two Input Signals."

2. For a = 1 (S_1, S_2 = 0 dB) the coefficients obtained by the computer program agree with those calculated from the special-case-equation (15) to within about 0.01 dB.

3. For small a values the 6.02-dB loss as suggested by Eq. (19) has been confirmed.

4. For all values of a, the calculated C_n values are in excellent agreement with experimentally obtained values. The experiment consists of the spectral analysis of the hard-limited summation of two sinusoids, as described in the section "Limiting of a Pair of Constant-Frequency CW Sinusoids."

The computer results are presented in two formats:

1. A set of curves for $C_n(a)$ with n values between -4 and 5 and with a values corresponding to the range from 0 to -30 dB, in Fig. 6.

2. Line spectra including a numerical printout for the C_n values in Fig. 7.

Both formats have their specific merits and drawbacks. The advantage of format 1 is to indicate clearly how the C_n values vary as a function of a. The drawing would be too crowded if one would attempt to display in it all higher order beat products, however. For this reason the presentation in format 2 was added. Figure 7 shows all beat products whose order is between -14 and 15 if they are stronger than -50 dB with respect to the total signal energy.

XTRAN Program for the Determination of $C_n(a)$:

```
D'N ARRAY(2,1024,1,1),I(3),M(256),SARRAY(256)
PI = 3.1415926535
NPG=8
* NTP = TØTAL NUMBER ØF DATA PØINTS, MAY BE SUBDIVIDED INTØ
  NG GRØUPS WITH NPG DATA PØINTS PER GRØUP
1  WRITE (1,11)
READ (0,12) NTP
NG = NTP/NPG
*EVALUATE THE FØRMULA FØR ALPHA
WRITE (1,13)
READ(0,17) AIA
A = EXP(ALØG(10.)/20.*(-AIA))
SI = SIN(2.*PI/NTP)
CØ = CØS(2.*PI/NTP)
DØ 200 J=1,NG
S = SIN(2.*PI/NG*(J-1))
C= CØS(2.*PI/NG*(J-1))
DØ 100 LL=1,NPG
IF (LL.EQ.1) GØTØ 50
STEMP = SI  *C+CØ *S
C = CØ  *C- SI *S
S = STEMP
50 DEN = SQRT(1.+ A*(A+2.*C))
ARRAY(1,NPG*(J-1)+LL,1,1) = (1.+A*C)/DEN
100  ARRAY(2,NPG*(J-1)+LL,1,1)=A*S/DEN
200 C'E
WRITE (1,14)
ANTP=NTP
I(1)= ALØG(ANTP)/ALØG(2.) +.1
FØR L=2,3: I(L)=0
CALL FASFT(ARRAY,I,M,SARRAY,-1,IFL)
WRITE (1,15)
DØ 500 N=MAXØ(NTP/2+1,NTP-15),NTP
X=ARRAY(1,N,1,1)
IF (ABS(X).LT..001) GØTØ500
WRITE(1,16) N-1-NTP,X,10.*ALØG10(X*X)
500 C'E
DØ 600 N=1,MINØ(NTP/2,15)
X= ARRAY(1,N,1,1)
IF(ABS(X).LT..001) GØTØ600
WRITE(1,16) N-1,X,10.*ALØG10(X*X)
600 C'E
WRITE (1,14)
G'Ø 1
11 F'T(3/,$SPECIFY TOTAL NUMBER ØF PØINTS : $,Z)
12 F'T (I4)
13 F'T (3/,$  A (MINUS DB) :  $,Z)
14 F'T (3/)
15 F'T (/,$ØRDER          CN          CN IN DB$,3/)
16 F'T(X,I3,4X,F10.4,5X,F9.2)
17 F'T(F5.2)
END
```

Security Classification

DOCUMENT CONTROL DATA - R & D

(Security classification of title, body of abstract and indexing annotation must be entered when the overall report is classified)

1. ORIGINATING ACTIVITY (Corporate author)	2a. REPORT SECURITY CLASSIFICATION
Naval Research Laboratory Washington, D.C. 20390	Unclassified 2b. GROUP

3. REPORT TITLE

CAPTURE AND SPURIOUS TARGET GENERATION DUE TO HARD LIMITING IN LARGE TIME-BANDWIDTH PRODUCT RADARS

4. DESCRIPTIVE NOTES (Type of report and inclusive dates)

Final report on the NRL Problem.

5. AUTHOR(S) (First name, middle initial, last name)

Hermann H. Woerrlein

6. REPORT DATE	7a. TOTAL NO. OF PAGES	7b. NO. OF REFS
December 22, 1969	48	8

8a. CONTRACT OR GRANT NO.	9a. ORIGINATOR'S REPORT NUMBER(S)
NRL Problem R02-38.201 b. PROJECT NO. S-4614-6173 c. d.	NRL Report 7001 9b. OTHER REPORT NO(S) (Any other numbers that may be assigned this report)

10. DISTRIBUTION STATEMENT

This document has been approved for public release and sale; its distribution is unlimited.

11. SUPPLEMENTARY NOTES	12. SPONSORING MILITARY ACTIVITY
	Department of the Navy (Naval Ship Systems Command), Washington, D.C. 20360

13. ABSTRACT

Hard limiting before pulse compression or correlation processing is a common approach to the CFAR (constant false alarm rate) problem, and it offers a good and simple solution in a single-target or scarce-target environment. With the advent of radars with a large time-bandwidth product the possibility arises that expanded radar returns due to multiple targets of interest may overlap very largely or entirely but still may be sufficiently separated to be resolved after receiver processing. In this case the compressed pulses cannot attain full amplitude at the processor output even if the signal-to-noise ratio at the input is very high; this phenomenon is known as capture and small signal suppression. The purpose of this report is to exhibit that, in addition to compressed target responses of reduced magnitudes, false targets may be generated with apparent amplitudes of the same order or exceeding those of legitimate targets. Spurious target generation in the case of chirp radar has been known for some time. The theory has been extended to maximum-length linear shift-register codes which are used as modulation functions of pulse-compression and phase-coded CW radars. It is found that a single pair of radar returns coded in this manner is subject to capture only and not to false target generation. Surprisingly, however, the addition of a third expanded signal produces a spurious response. This generation of a false target should be taken in account when the dynamic range of future phase-coded radars using linear shift-register codes is specified, in particular if the radar is designed for automatic track and raid-size determination.

(OVER)

14 KEY WORDS	LINK A		LINK B		LINK C	
	ROLE	WT	ROLE	WT	ROLE	WT
Radar						
Hard limiting						
Pulse compression						
CFAR						
False targets						
Ghost targets						
Capture						
Phase-coded radar signals						
Theory						

General formulas were derived to predict the effects of capture and false target generation as a function of the signal energy distribution and relative phasing before entering the limiting device. The formulas were evaluated numerically, with the results being presented in the form of computer-generated plots.